Thermal Engineering Issues in Hydrogen Storage for Mobile and Portable Applications

S. SRINIVASA MURTHY

Professor of Refrigeration & Clean Energy Technologies

Fourth Indo-US Round Table on
ALTERNATE ENERGY
September 21-23, 2010
NIAS - IISc, Bangalore, India

Department of Mechanical Engineering
Indian Institute of Technology Madras
Chennai - India

Report Documentation Page

Form Approved
OMB No. 0704-0188

1. REPORT DATE	2. REPORT TYPE	3. DATES COVERED
SEP 2010	**N/A**	**-**

4. TITLE AND SUBTITLE	5a. CONTRACT NUMBER
Thermal Engineering Issues in Hydrogen Storage for Mobile and Portable Applications	5b. GRANT NUMBER
	5c. PROGRAM ELEMENT NUMBER
6. AUTHOR(S)	5d. PROJECT NUMBER
	5e. TASK NUMBER
	5f. WORK UNIT NUMBER
7. PERFORMING ORGANIZATION NAME(S) AND ADDRESS(ES) **Department of Mechanical Engineering Indian Institute of Technology Madras Chennai, India**	8. PERFORMING ORGANIZATION REPORT NUMBER
9. SPONSORING/MONITORING AGENCY NAME(S) AND ADDRESS(ES)	10. SPONSOR/MONITOR'S ACRONYM(S)
	11. SPONSOR/MONITOR'S REPORT NUMBER(S)

12. DISTRIBUTION/AVAILABILITY STATEMENT
Approved for public release, distribution unlimited

13. SUPPLEMENTARY NOTES
See also ADA560467. Indo-US Science and Technology Round Table Meeting (4th Annual) - Power Energy and Cognitive Science Held in Bangalore, India on September 21-23, 2010. U.S. Government or Federal Purpose Rights License

14. ABSTRACT

15. SUBJECT TERMS

16. SECURITY CLASSIFICATION OF:			17. LIMITATION OF ABSTRACT	18. NUMBER OF PAGES	19a. NAME OF RESPONSIBLE PERSON
a. REPORT	b. ABSTRACT	c. THIS PAGE			
unclassified	**unclassified**	**unclassified**	**SAR**	**82**	

ACKNOWLEDGEMENTS

Thanks are due to my colleague
•Prof. M.P.Maiya
Graduate students
•Dr.E. Anil Kumar, Dr.G. Mohan, Dr.Muthukumar
for their contribution to the results presented in this paper.

And to the support of the following are gratefully acknowledged:
•Department of Science & Technology, Govt. of India.
•Ministry of New & Renewable Energy, Govt. of India.
•United States Department of Energy, Office of Energy Efficiency & Renewable Energy – Fuel Cell Technologies Program Office through Argonne National Laboratory.
•U.S. Army Communications - Electronics Research, Development and Engineering Center and International Technology Center, Pacific.

PRESENTATION FORMAT

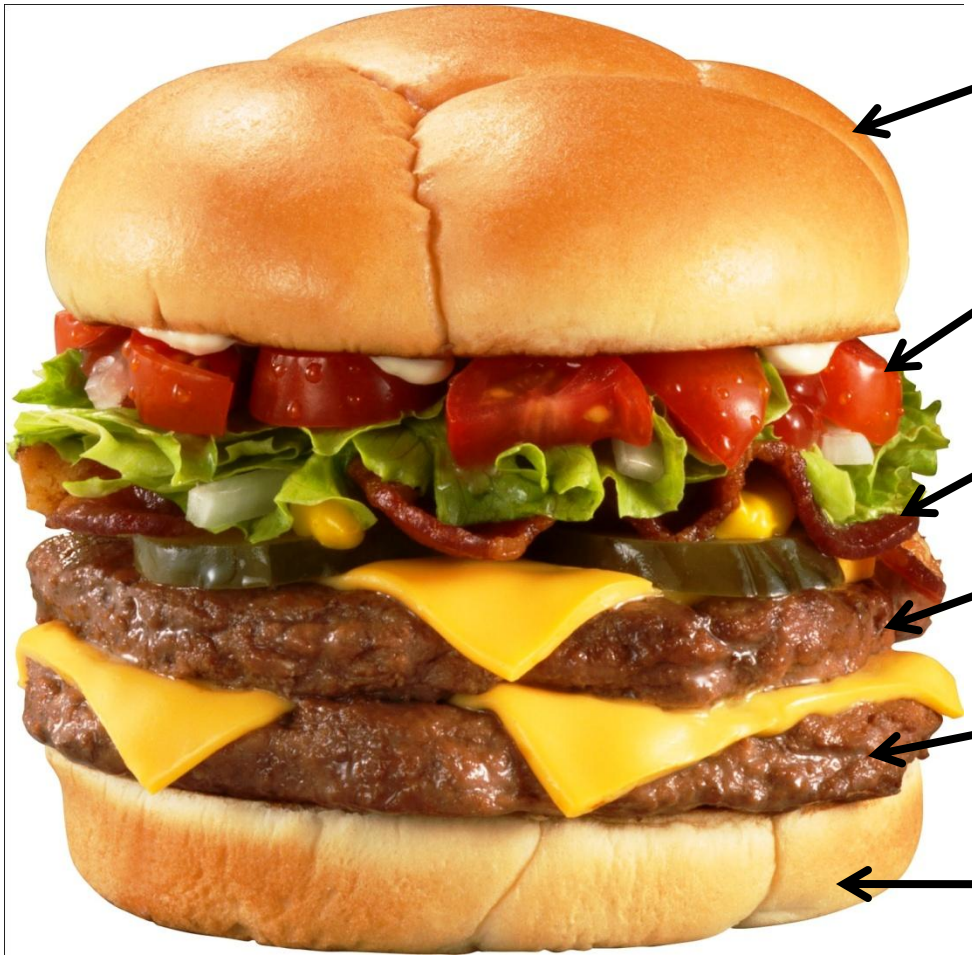

INTRODUCTION TO HYDROGEN STORAGE

SIMULATION & DESIGN ISSUES

THERMODYNAMIC PROPERTIES

THERMOPHYSICAL PROPERTIES

ISSUES RELATED TO NEW MATERIALS

CHALLENGES & CONCLUDING REMARKS

HYDROGEN STORAGE OPTIONS:

Compressed Gas →

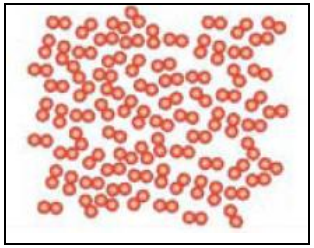

→ Heavy storage tanks
Very high pressures
High Compression energy
Explosion risk

Cryogenic Liquid →

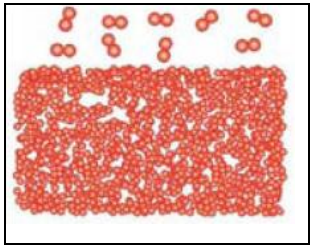

→ Heavy plant investment
Highly energy intensive
Losses due to boil-off

Solid State Storage

- **Physisorption** →

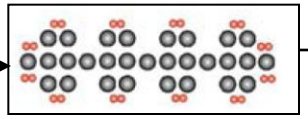

→ Good hydrogen capacity
Good recyclability
Temp. limitations

- **Chemisorption** →

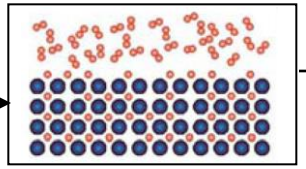

→ Medium hydrogen capacity
Good recyclability

- **Complex hydrides** →

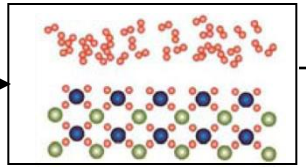

→ High hydrogen capacity
Low recyclability

In physisorption, molecular hydrogen is adsorbed by intermolecular (van der Walls) forces. Carbons, organic & inorganic frameworks are the examples.

In chemisorption, hydrogen molecules and chemical bonding of hydrogen atoms dissociate by integration in the lattice of a metal or an alloy, or by formation of a new compound. Metal hydrides, chemical hydrides and complex hydrides are the examples.

A given material can exhibit both physi- and chemi-sorption at certain stages of sorption process.

Chemisorption may provide higher volumetric and gravimetric storage capacities, but the chemical bonds need to be split or recombined.

Physisorption is not subject to this constraint as hydrogen stays in molecular form.

One of the major differences between physisorption and chemisorption is their 'binding energies'.

Physisorption bonding is usually too weak (< 10 kJ/mol) thus demands very low temperatures for significant storage capacity.

Chemisorption shows too high stability (> 50 kJ/mol) demanding high desorption temperatures.

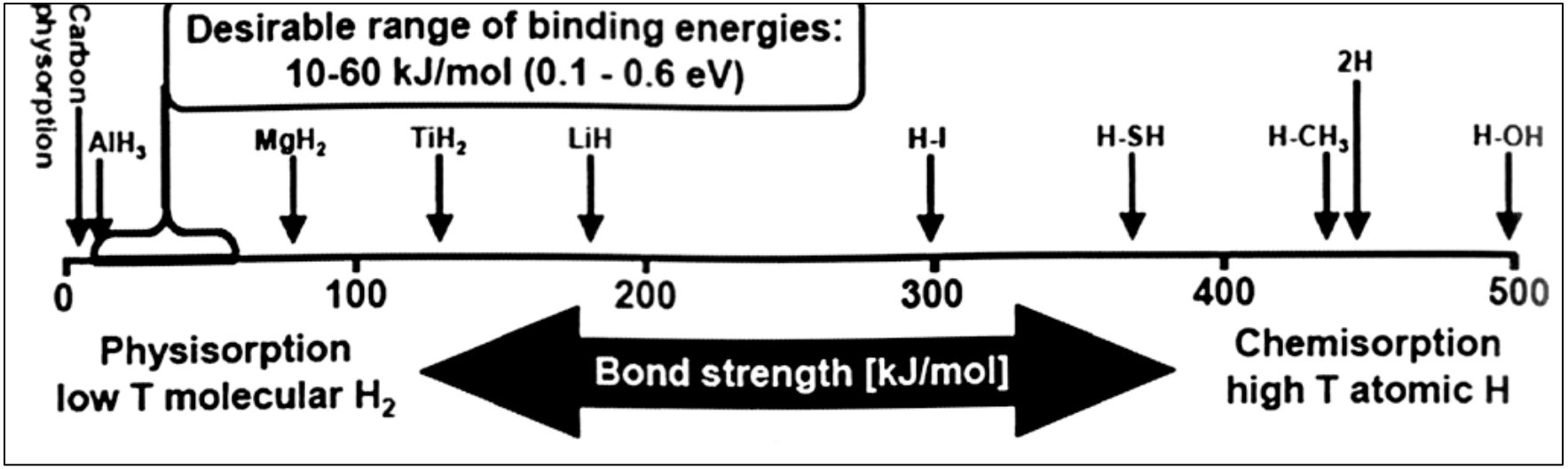

Bond strengths for physisorption and chemisorption and the desirable range of binding energies that allow hydrogen release at about room temperatures.

V.Berube, G.Radtke,M.Dresselhaus, G.Chen; Int. Jr. Energy Res., 31, p.207, 2007

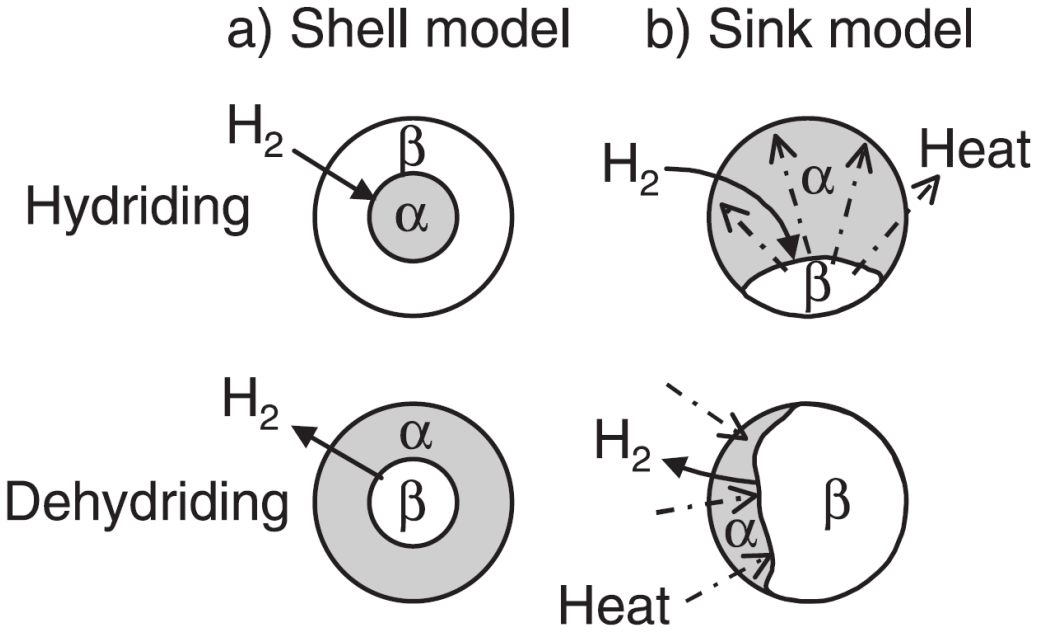

Two adsorption models, on the left the shell model that applies to large magnesium particles where so much nucleations occur that a closed hydride layer forms that hinders further hydriding at a certain stage.

On the right the sink model that applies to small particles (smaller than 75 *μm) wherein only one hydride nucleation occurs due to* the heat which neutralizes the other nucleation center. The nucleus acts as a sink which removes the hydrogen atoms before they can initiate a new nucleation elsewhere.

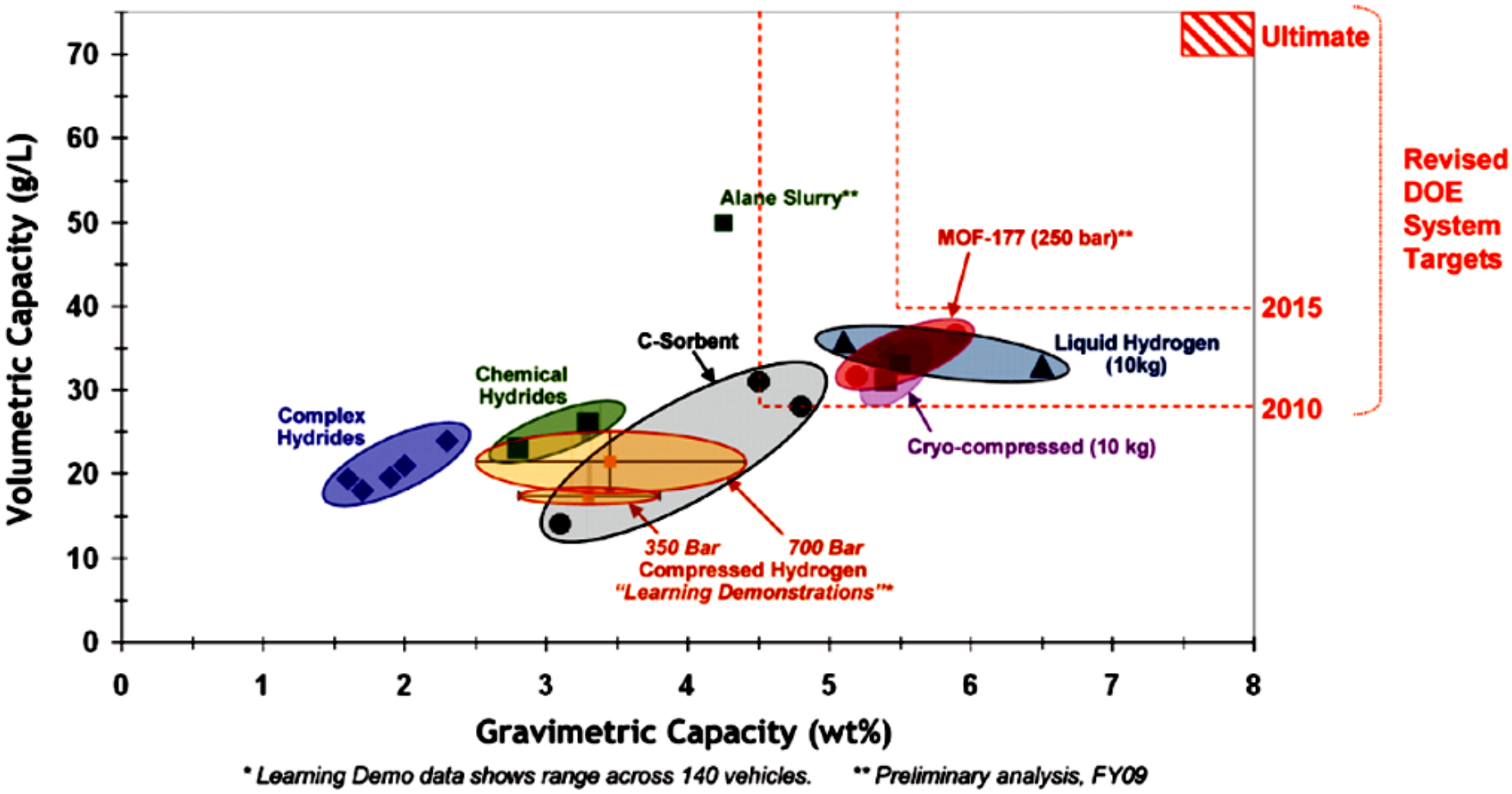

"In 2009, storage targets were revised and the three Storage Centers of Excellence continued to make progress in the down-selection of materials"

Source: US DoE

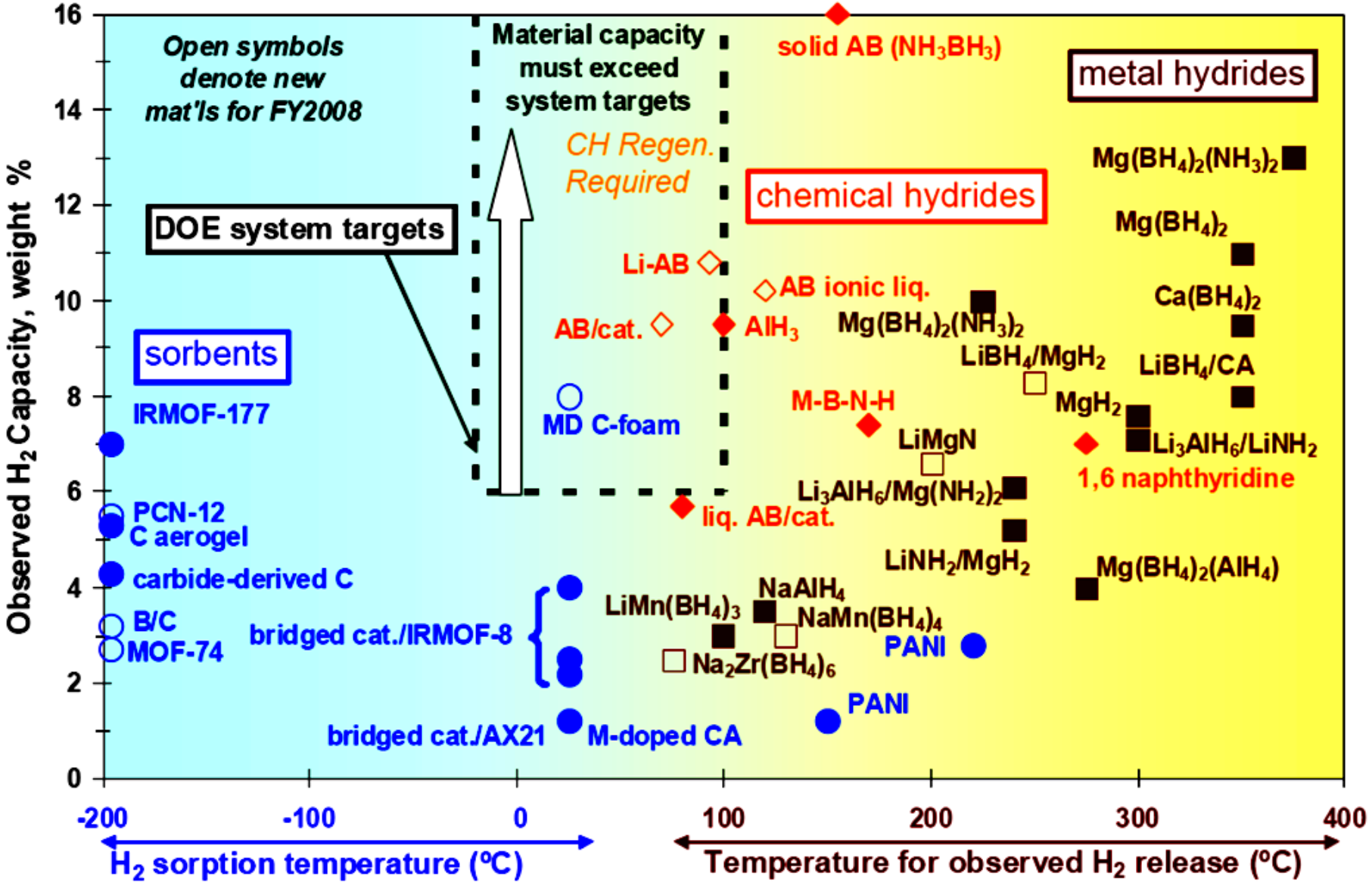

Current State of the Art, Figures by DOE: G. Thomas (2007), G. Sandrock (2008) Presentation "Hydrogen Storage" by Sunita Satyapal, 2008 DOE Hydrogen Program Merit Review and Peer Evaluation Meeting June 9, 2008.

Capacity Type	2010 Targets	2015 Targets
Gravimetric, *system* (kg H_2 / kg system)	6.0	9.0
Gravimetric, *material* (kg H_2 / kg system)	12.0	18.0
Volumetric, *system* (kg H_2 / L system)	0.045	0.080
Volumetric, *material* (kg H_2 / L system)	0.090	0.160

Original US Department of Energy capacity targets are shown above. The material capacities are assumed to be 2 times larger than the system capacities. These were modified in February 2009 and the new US DOE are shown below.

Capacity Type	2010 Targets	2015 Targets
Gravimetric, *system* (kg H_2 / kg system)	4.5	5.5
Gravimetric, *material* (kg H_2 / kg system)	9.0	11.0
Volumetric, *system* (kg H_2 / L system)	0.028	0.040
Volumetric, *material* (kg H_2 / L system)	0.056	0.080

ON-BOARD REVERSIBLE HYDRIDE MATERIALS

These include the various metal hydrides, some of the complex metal hydrides, amides, etc that release hydrogen endothermically.

Endothermic release allows for thermodynamically favorable, exothermic rehydrogenation during on-board recharging of the hydrogen storage materials under reasonable temperature (< 300°C) and pressure (< 200 bar) conditions.

Physisorption materials involve weakly bound molecular hydrogen that is on-board reversible but generally require operating at liquid nitrogen temperatures.

OFF-BOARD REGENERABLE HYDRIDE MATERIALS

These either release hydrogen exothermically, and/or involve complex chemical regeneration schemes that cannot be performed on board a vehicle. Hydrocarbons, ammonia borane, and alane are typical examples.

The hydrocarbons and alane release hydrogen endothermically, but high hydrogen pressures or the complexity of their rehydrogenation most likely will require an off board process.

Ammonia borane and other materials that release hydrogen rather exothermically cannot be rehydrogenated readily at common pressures and temperatures.

TYPES OF METAL HYDRIDES

- **AB type (Ti based)**

Favourable P-C-T and thermodynamic properties, slow activation and sensitivity to impurities in hydrogen gas

- **AB_2 type (Zr based)**

Favourable P-C-T properties, large sloping plateau, high hysteresis, less cyclic stability and difficult to produce on commercial level

- **A_2B type (Mg based)**

High hydrogen capacity, the hydrogen desorption temperatures are high and kinetics is poor

- **AB_5 type (Rare earth based)**

Favourable P-C-T, thermodynamic, kinetic properties, easy activation, cyclic stability and resistance to impurities in hydrogen gas

TYPICAL METAL HYDRIDES

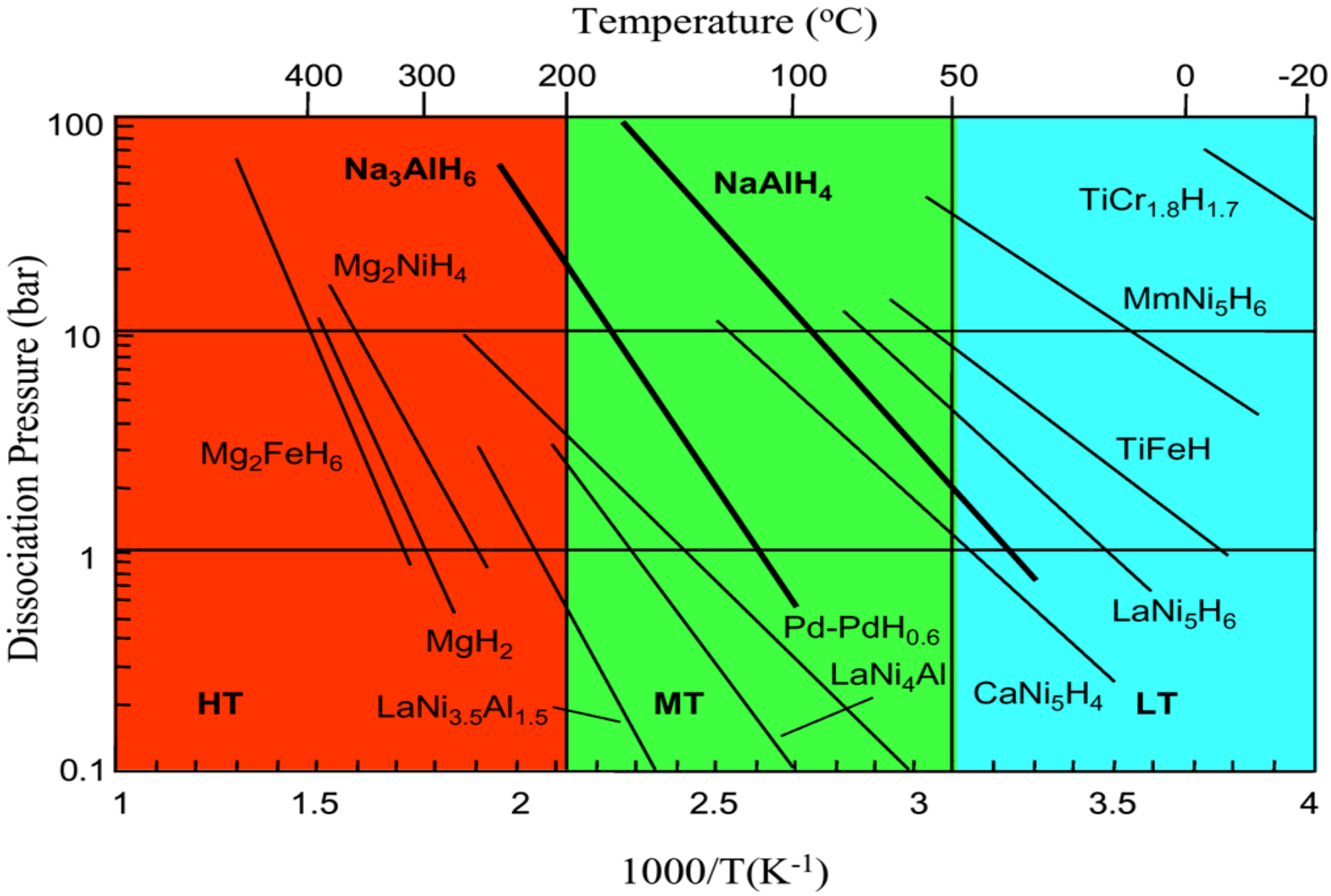

SOLID STATE HYDROGEN STORAGE DEVICES

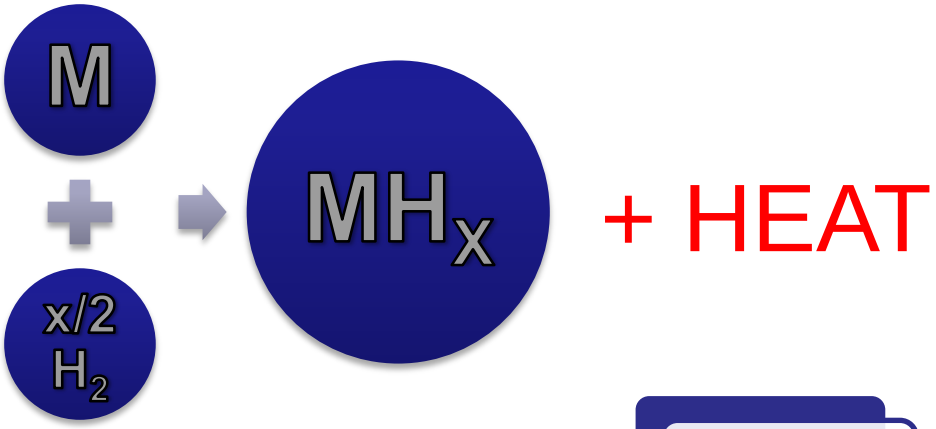

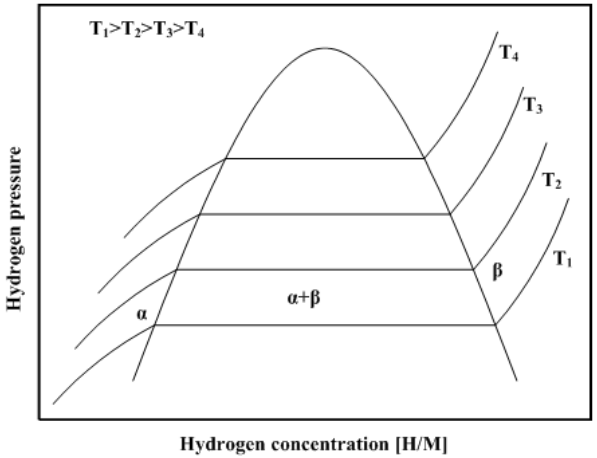

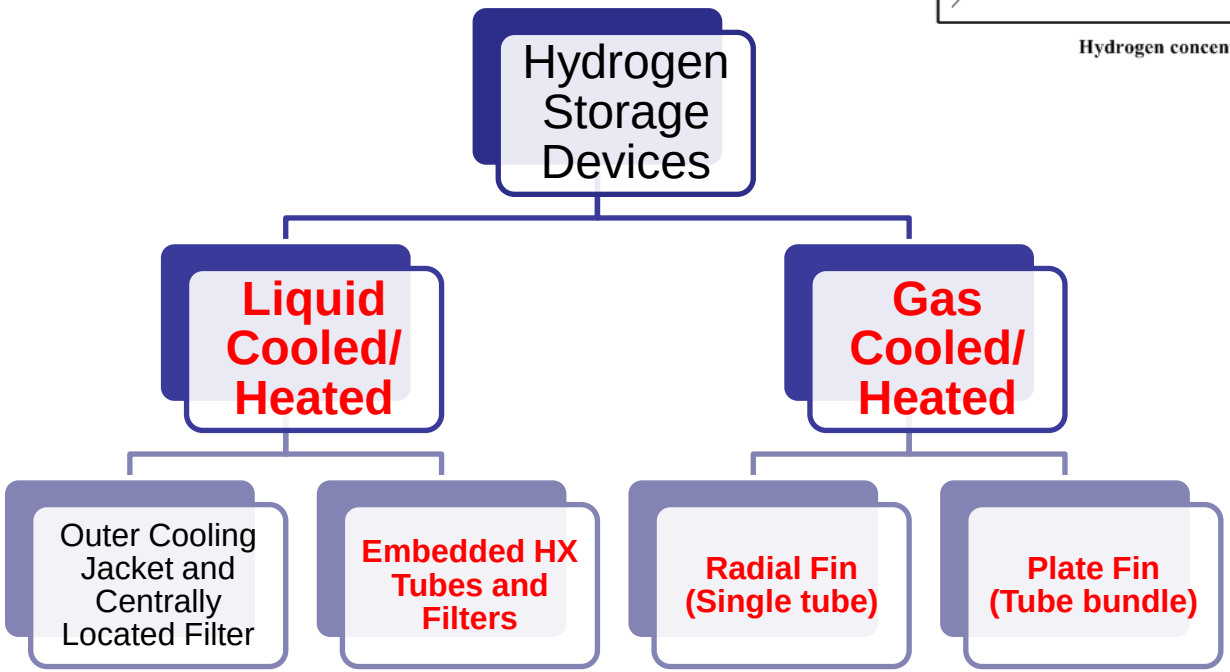

THERMAL ENGINEERING ISSUES

- **Heat transfer is the major sorption/desorption rate controlling factor in metal hydride beds.**
  - **In order reduce the cycle time and to reduce the total weight, improvement in the heat transfer characteristics of the bed is the most desirable.**
  - **The hydriding and dehydriding reactions occur in the entire bed. However, faster rate of reaction may be observed in a narrow region close to the heat transfer boundary.**
- **Reactor configuration and geometric parameters are important in obtaining the desired sorption / desorption performance from hydrogen storage devices.**
- **Hydrogen supply pressure and coolant temperature are important operating parameters in deciding the charging / discharging rates in hydride devices.**
- **While storage material properties (Sorption, Thermodynamic, Thermophysical) are important, the thermal design of the overall storage device is crucial.**
- **Thermal masses of the heat transfer tubes, container, filters, distributors, heat transfer fluid, etc have to be minimized.**

Physical Models recently studied by the Author

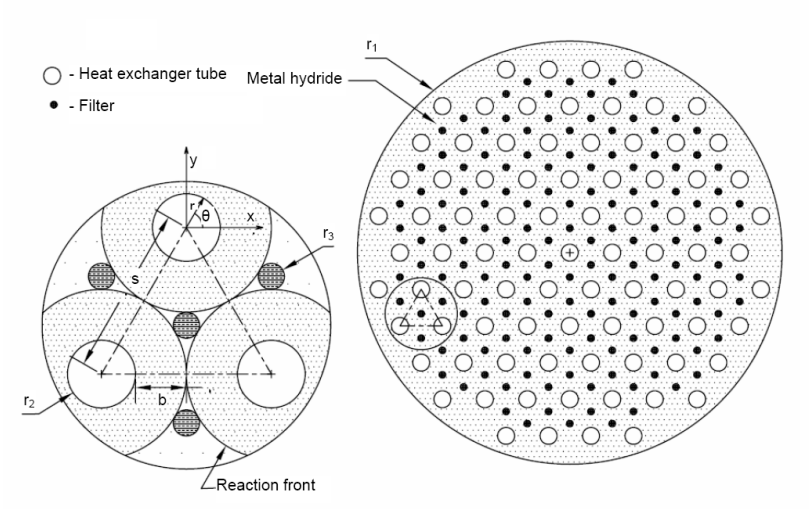

Liquid Cooled Hydrogen Storage Device with Embedded Heat Exchanger Tubes

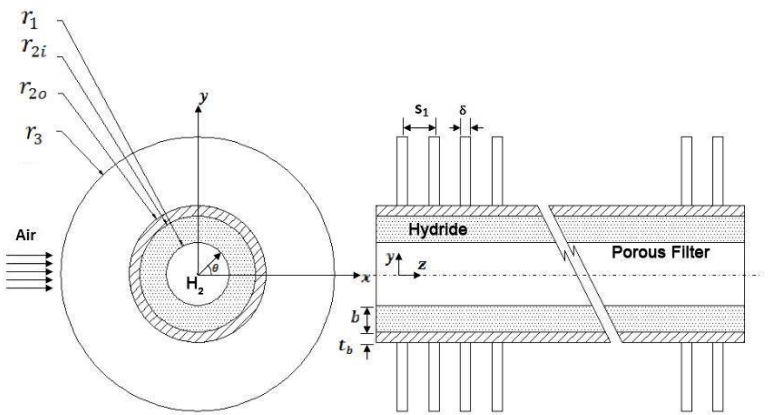

Hydrogen Storage Device with Radial Fins

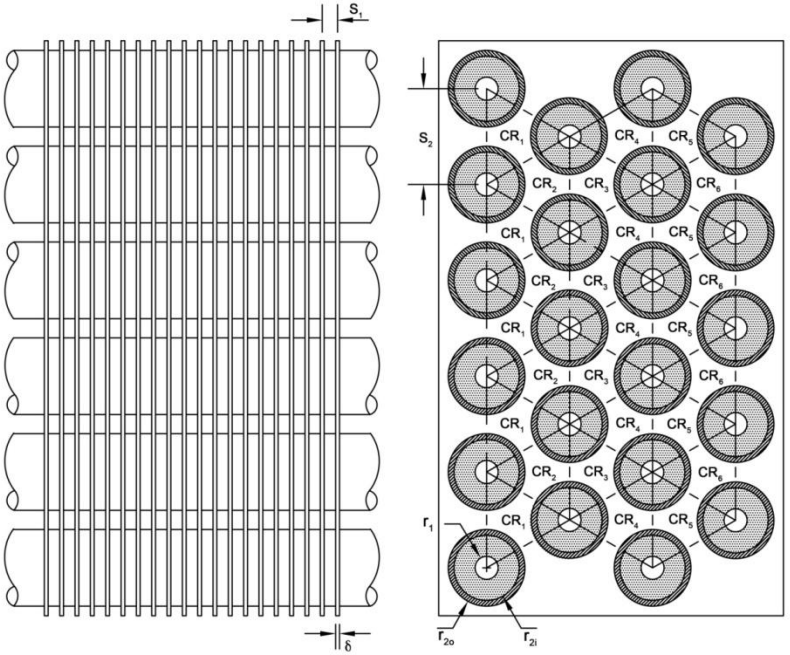

Hydrogen Storage Device with Plate Fins

Computational Models used in COMSOL Multiphysics™

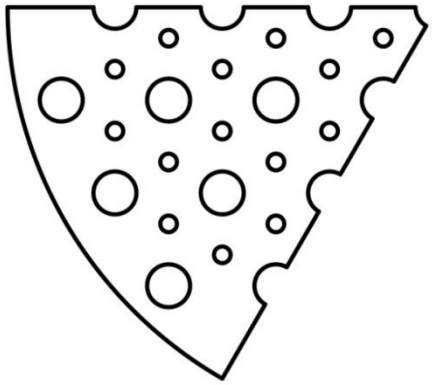

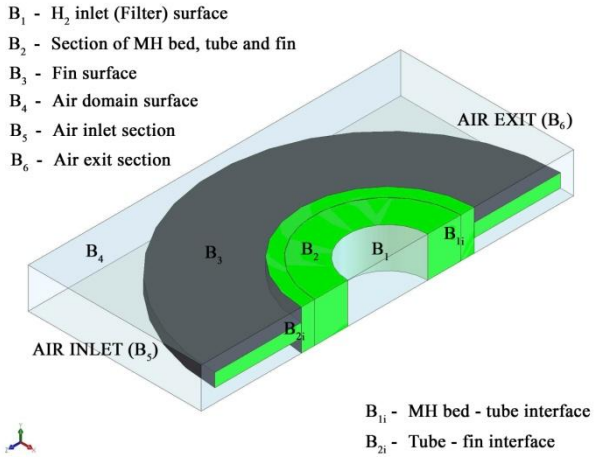

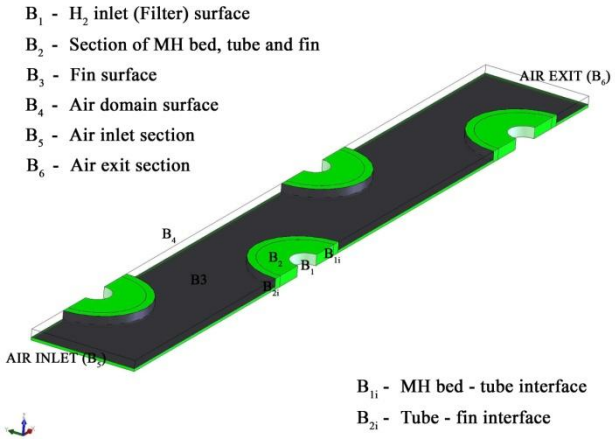

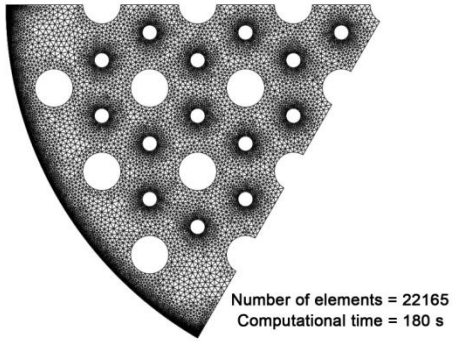

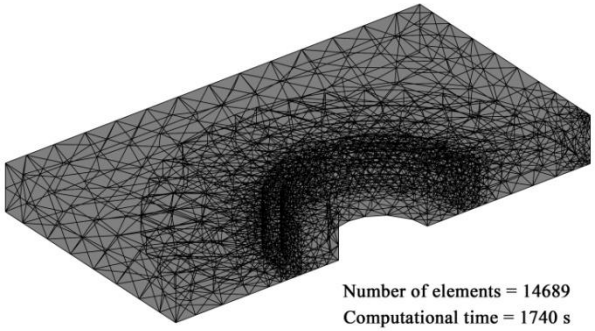

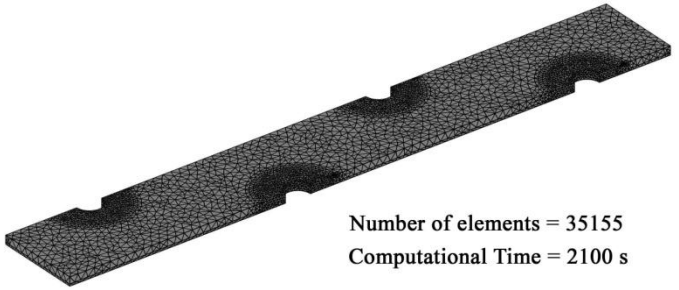

Liquid Cooled Storage Device

Air Cooled Storage Device with Radial Fins

Air Cooled Storage Device with Plate Fins

Minimization of Total Weight

Example

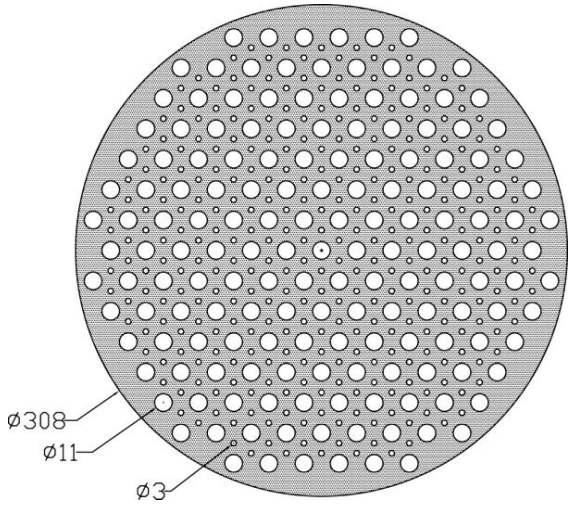

Data

Charging capacity	**= 2 kg**
Charge level	**= 80 %**
Charge time	**= 300 s**
Supply pressure	**= 15 bar**
Coolant Temperature	**= 300 K**
L/D ratio	**= 2 – 4**
Hydriding alloy	**= $LaNi_5$**

Results

Radius of container (r_1)	**= 154 mm**
Radius of HX tube (r_2)	**= 5.5 mm**
Radius of filter (r_3)	**= 1.5 mm**
Pitch distance (s)	**= 22 mm**
Total no. of HX tubes	**= 163**
Total no. of filters	**= 282**
Length of device (L)	**= 986 mm**
L/D of device	**= 3.2**
A_{sc}/V_c of device	**= 1.182 cm^2/cm^3**
Total system weight (W_t)	**= 370 kg**

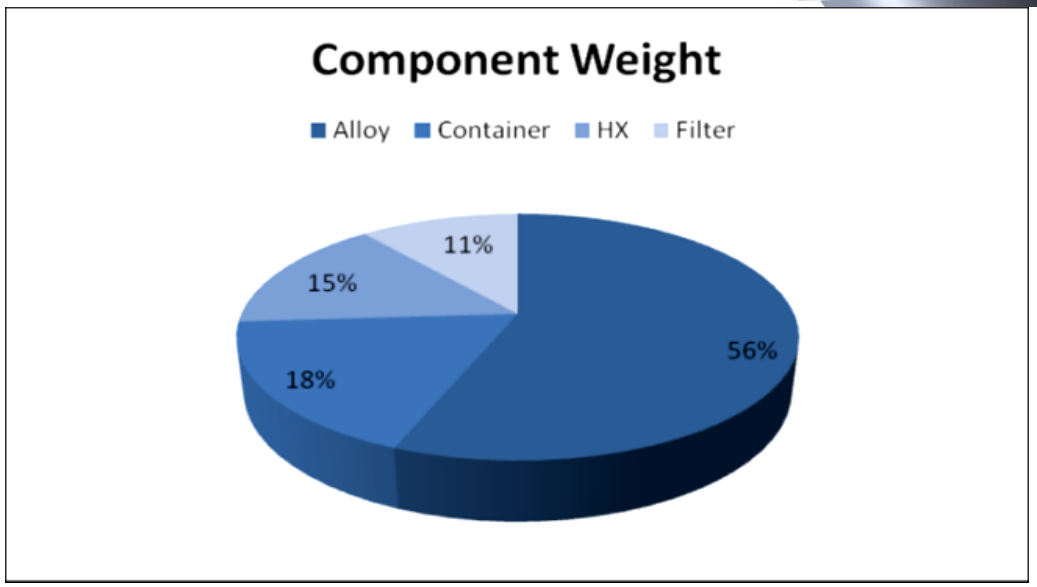

Results on Air Cooled Devices with Radial Fins

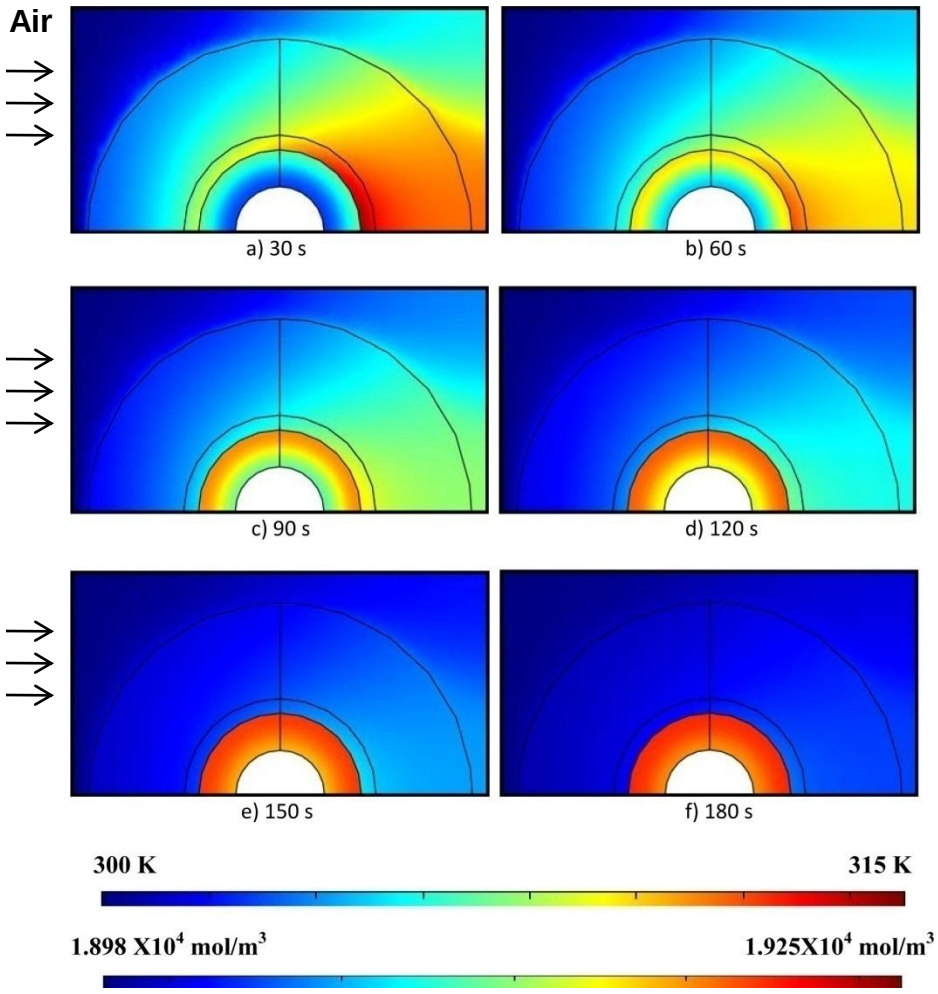

Formation of hydride inside tubular storage device with fins kept within the air stream during absorption at different time intervals (b=5 mm, p=15 bar, T_f=300 K)

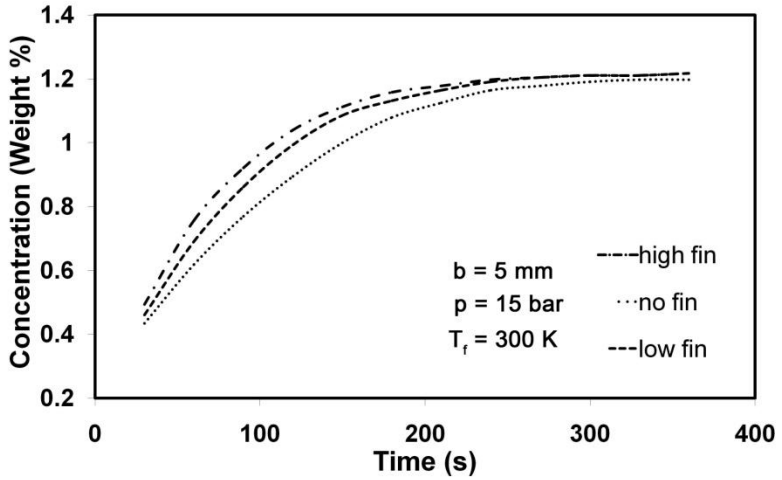

Effect of external fins on rate of hydriding

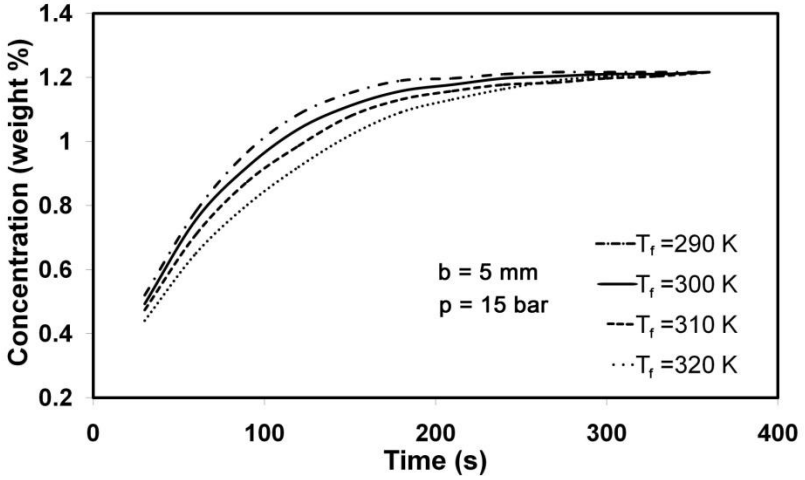

Effect of air temperature on hydride formation

Results on Air Cooled Devices with Tube Bundle

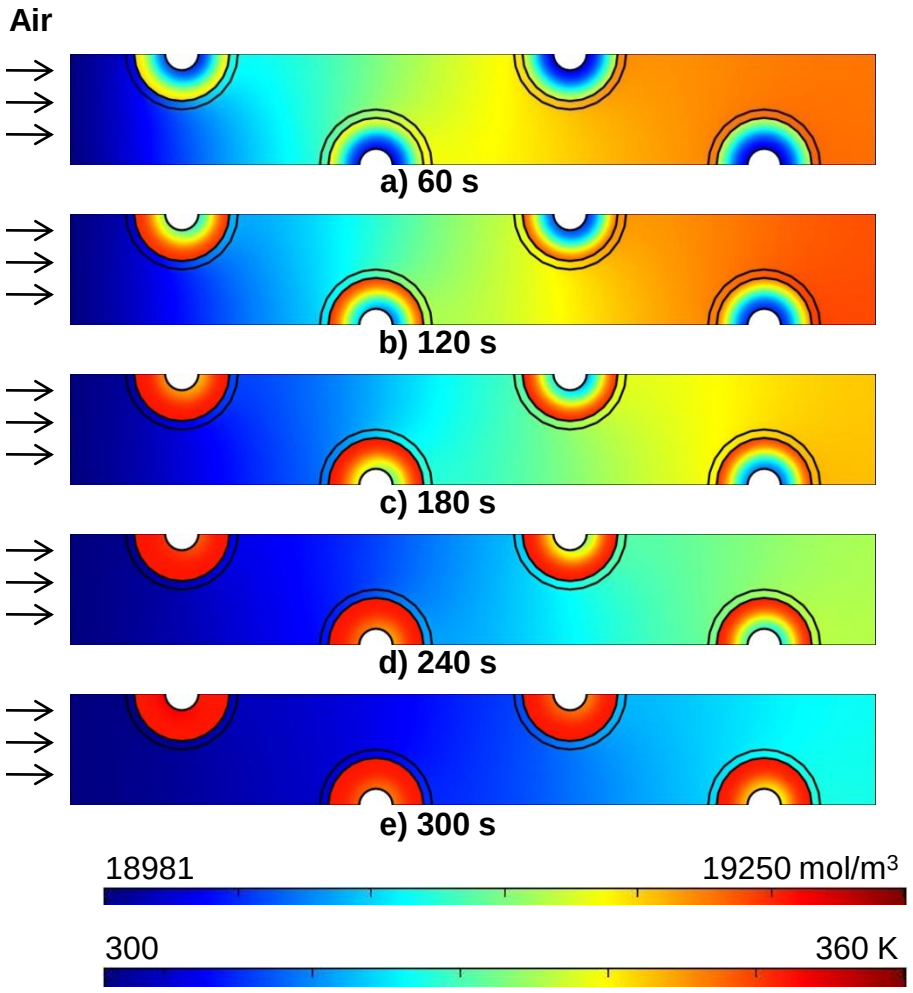

Temperature profile of air and concentration profile of hydride bed for the finned-tube metal hydride storage device at different time intervals (p=15 bar, T_f=300 K, s/d=2, b=5.5 mm, u= 1 m/s)

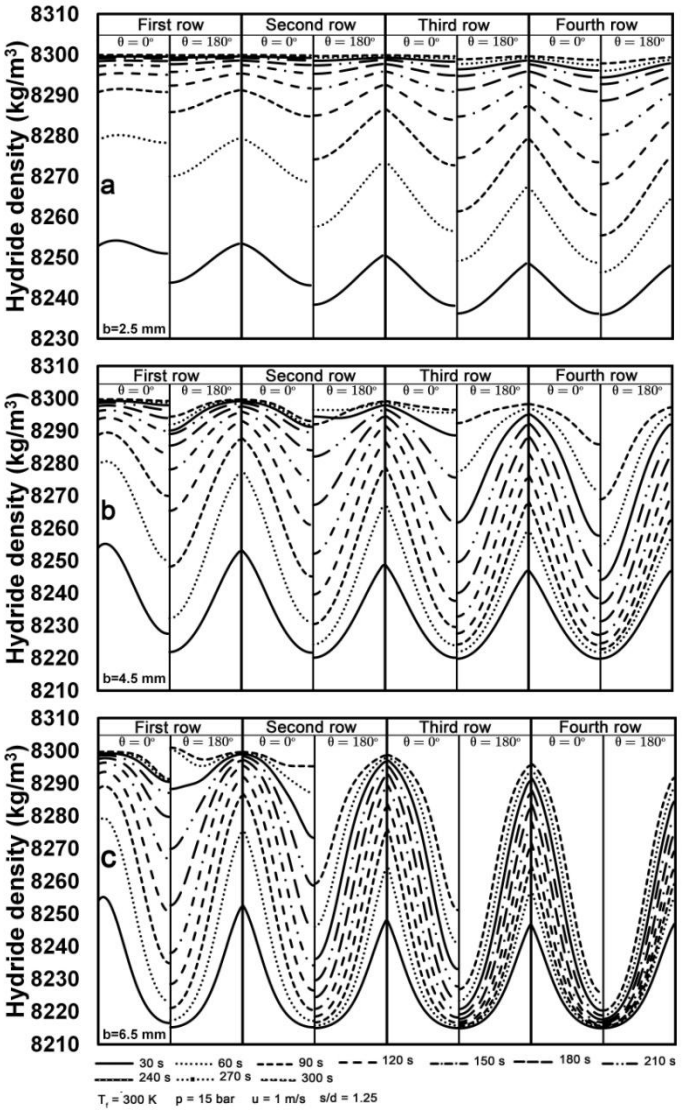

Variation of hydride density at leading and trailing cross sections at different bed thicknesses

Observations

Liquid Cooled Devices

- **Among the geometric parameters, bed thickness, cooling tube diameter and pitch distance are important in controlling the hydrogen sorption rate where as scaling factor (r_1/s) does not show significant influence.**
- **Hydrogen supply pressure and coolant temperature are important operating parameters which control the sorption rate in metal hydride devices.**
- **Devices with thinner beds exhibit faster kinetics, i.e., hydrides are formed at faster rate. However, for given storage capacity and charging rate, these are heavier.**
- **Pitch distance is the main characteristic parameter which controls the total system weight and charging time.**
- **Corresponding to each bed thickness, an optimum HX tube size could be determined for the lowest system weight.**
- **Device at higher final charging levels need more charging time. Obviously it contains lesser quantity of hydriding alloy.**
- **Storage devices with thin beds have high L/D ratio for a given scaling factor.**
- **Corresponding to specified storage capacity and rate, r_1/s determines the container diameter and length to fit into a specified application. Number of HX tubes and filters are also decided based on this factor.**

Observations …. continued

Air Cooled Devices

Conclusions common to both configurations

- **Air cooled storage devices with fins show significant improvement in sorption over the ones without fin emphasizing the importance of external heat transfer. However performance improvement of high finned tubes over low finned tubes is small.**

- **Spatial variation in sorption rate exists in the annular hydride bed and among successive rows down-stream in a tube bundle.**

- **Low gas temperature, high gas velocity and high thermal conductivity of bed improve the sorption performance of the device.**

Device with bundle of tubes

- **The rate of hydrogenation of the device is affected by the combined influence of bed thickness and s/d ratio, indicative of the mutual correlation between hydride bed heat transfer and convective transport of the rejected heat.**

- **External heat transfer augmentation by the variation of s/d ratio is more pronounced in devices with thicker hydride beds.**

- **As hydriding rate decreases progressively for successive tube rows down-stream of the flow, number of tube rows in a bundle should be reduced to the minimum so as to improve the sorption rate.**

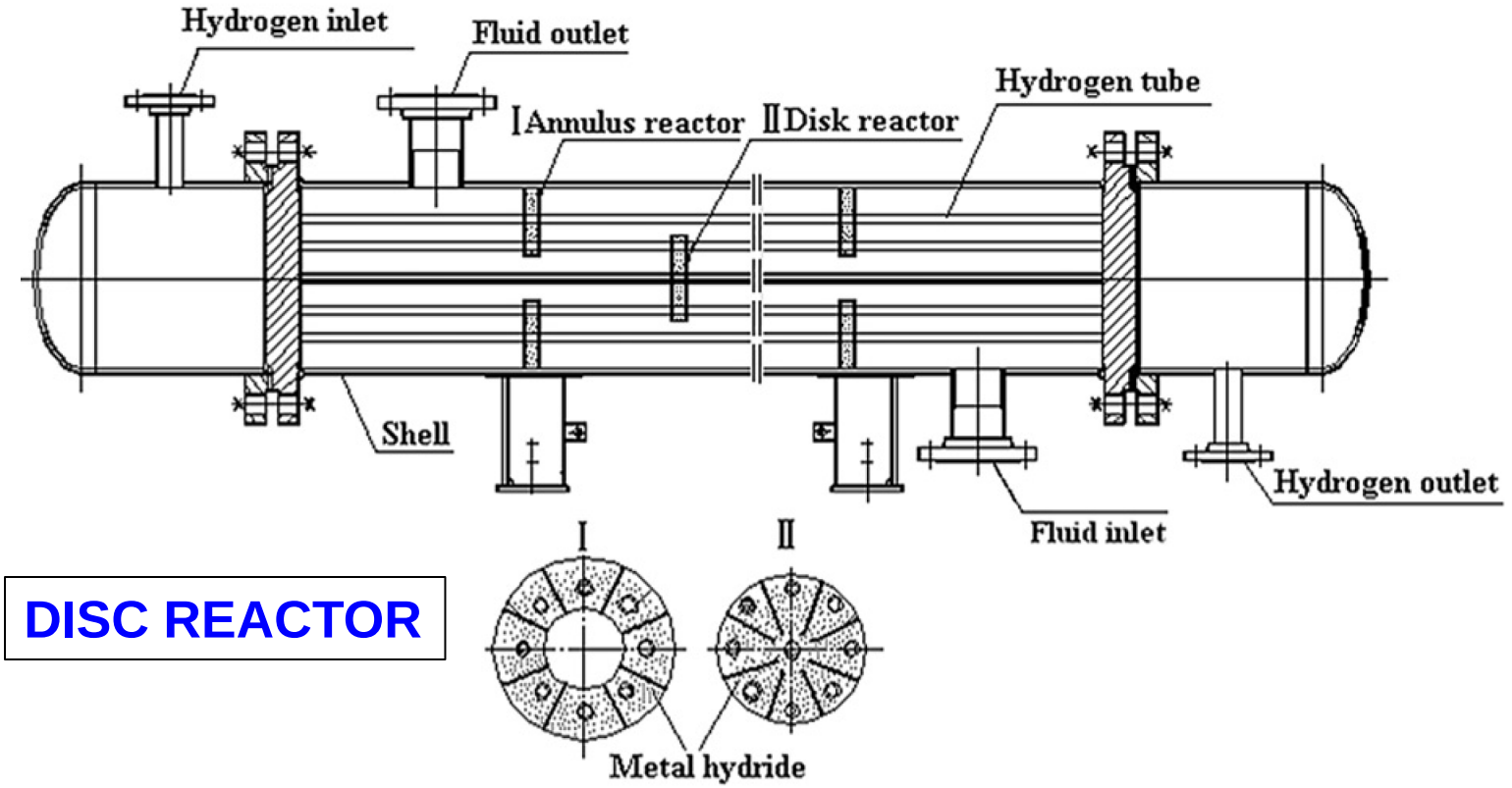

DISC REACTOR

In the annulus-disc reactor proposed by Wang et al. as shown in Figure, MH is packed in the annulus/disc units and hydrogen flows in the tubes which penetrate through the units and enable mass transfer with MH in the radial direction.

Heat transfer simultaneously takes place over the external surfaces of disc units. The capacity of this type of reactor can be adjusted within a large range by varying the number of disc units.

Meanwhile, a fast reaction rate was obtained by properly adjusting the dimension and distance of disc units.

Wang YQ, Yang FS, Zhang ZX, Feng X, Guo QF. Design and process simulation of metal hydride reactors Journal of Xi'an Jiaotong University 2006;40:831–5.

MEASUREMENT OF P-C-T CHARACTERISTICS

Gravimetric method

In gravimetric method, the hydrogen absorption is measured by monitoring the mass of the sample with a step change in the hydrogen pressure and requires relatively sensitive instrumentation.

Volumetric method

In volumetric method the hydrogen sorption or uptake is measured by monitoring the drop in hydrogen pressure in a system of a fixed, known volume, with desorption being monitored by an increase in pressure.

This can be further classified as

Static P-C-T measurement method

In static measurement a given amount of hydrogen is stepwise added or withdrawn from the system. At the end of each step, equilibrium condition is established.

Dynamic P-C-T measurement method

In dynamic P-C-T curve measuring method a constant hydrogen mass flow rate is maintained and amount absorbed or desorbed is monitored with respect to pressure.

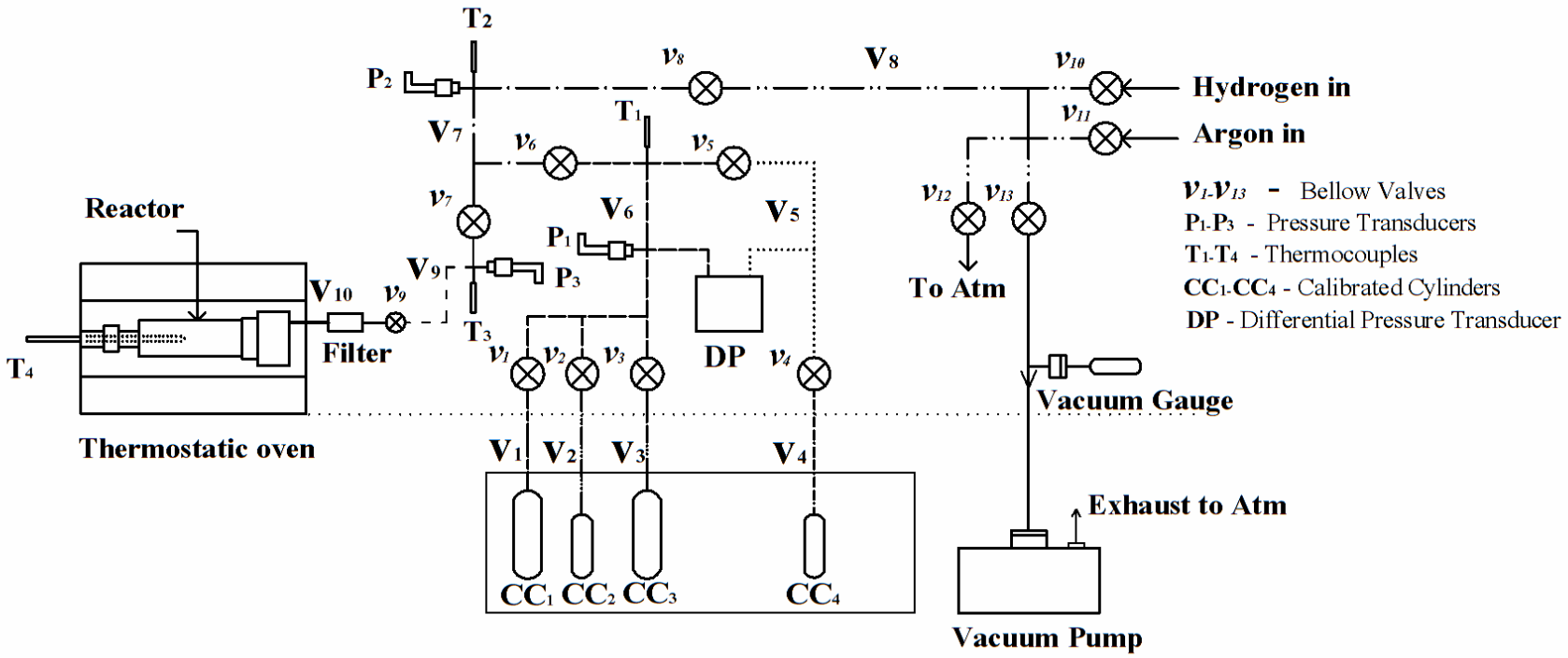

Experimental setup for static P-C-T measurements

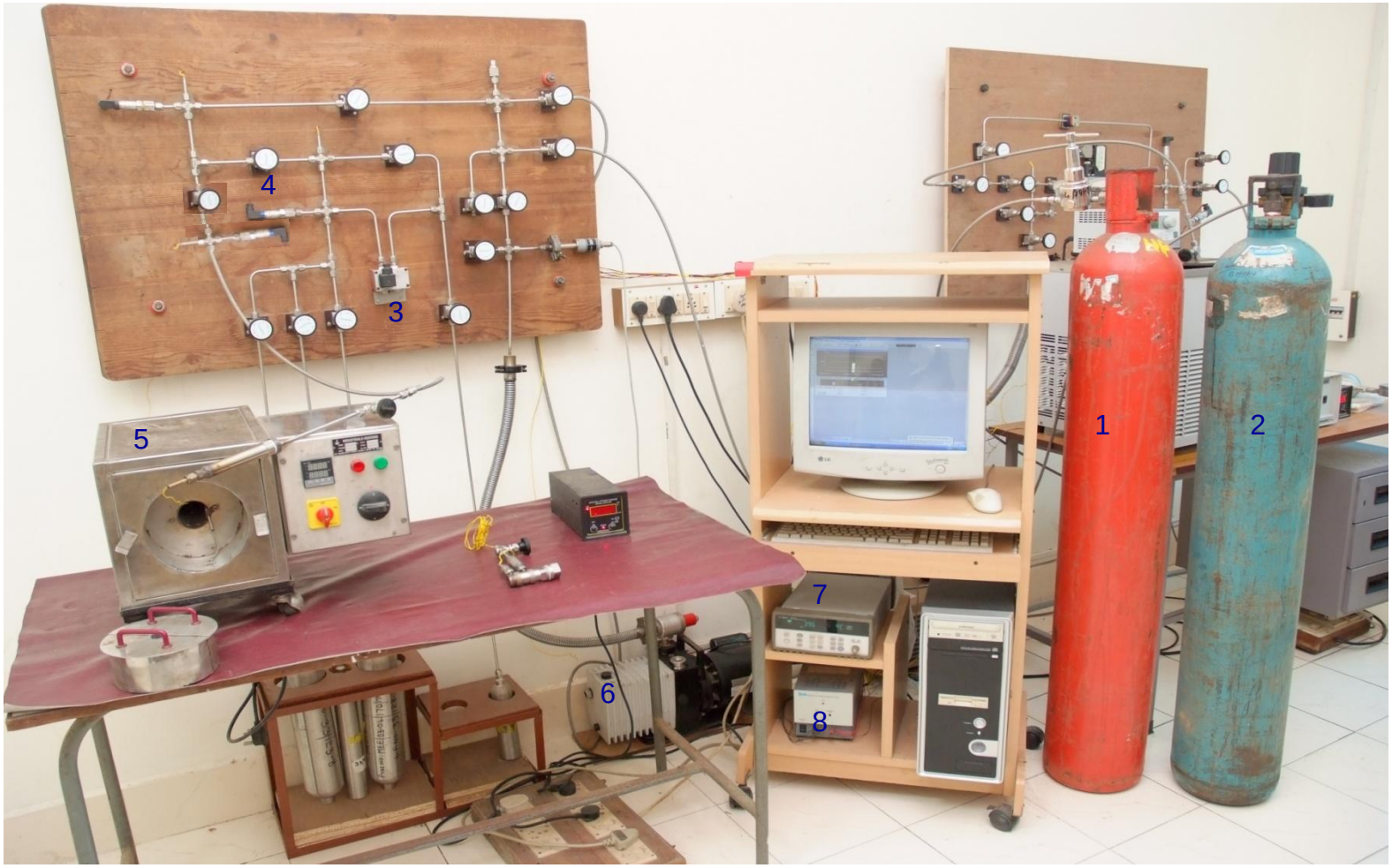

1.Hydrogen cylinder **2.Argon cylinder** **3. Differential Pressure Transducer**
4. Pressure Transducer **5. Oven** **6. Vacuum Pump**
7. Data logger **8.Calibrated Cylinders**

Experimental Setup for static P-C-T measurements

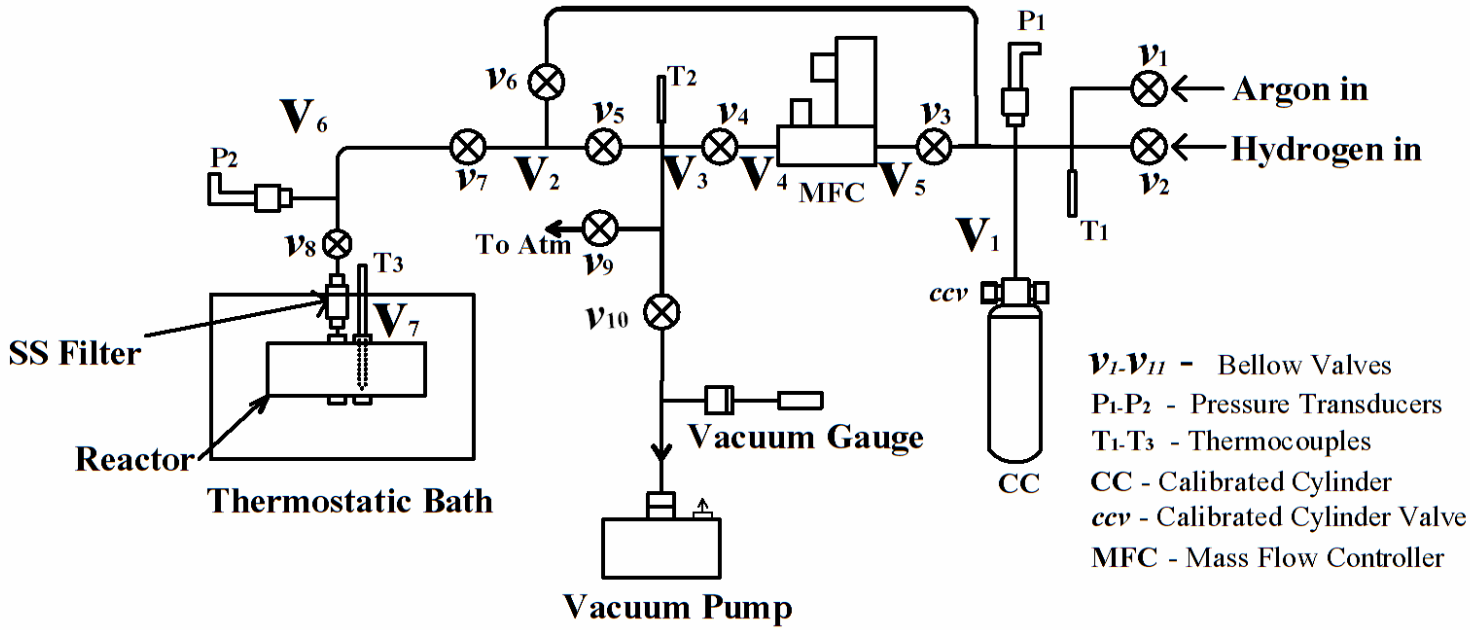

V1, Volume of **CC** and pipe volume between *ccv*, v_1, v_2, v_3 and v_6

V2, Volume of pipe between v_5, v_6 *and* v_7

V3, Volume of pipe between v_4, v_5, v_9, v_{10} and v_{11}

V4, Volume of pipe between v_4 and MFC

V5, Volume of pipe between v_3 and MFC

V6, Volume of pipe between v_7 and v_8

V7, Free volume in the reactor up to valve v_8

Experimental setup for dynamic P-C-T measurements

1. Vacuum pump 2. Thermostatic bath 3. MFC 4. Calibrated cylinder
5. Argon cylinder 6. Hydrogen cylinder 7. Data logger

Experimental setup for dynamic P-C-T characteristics measurements

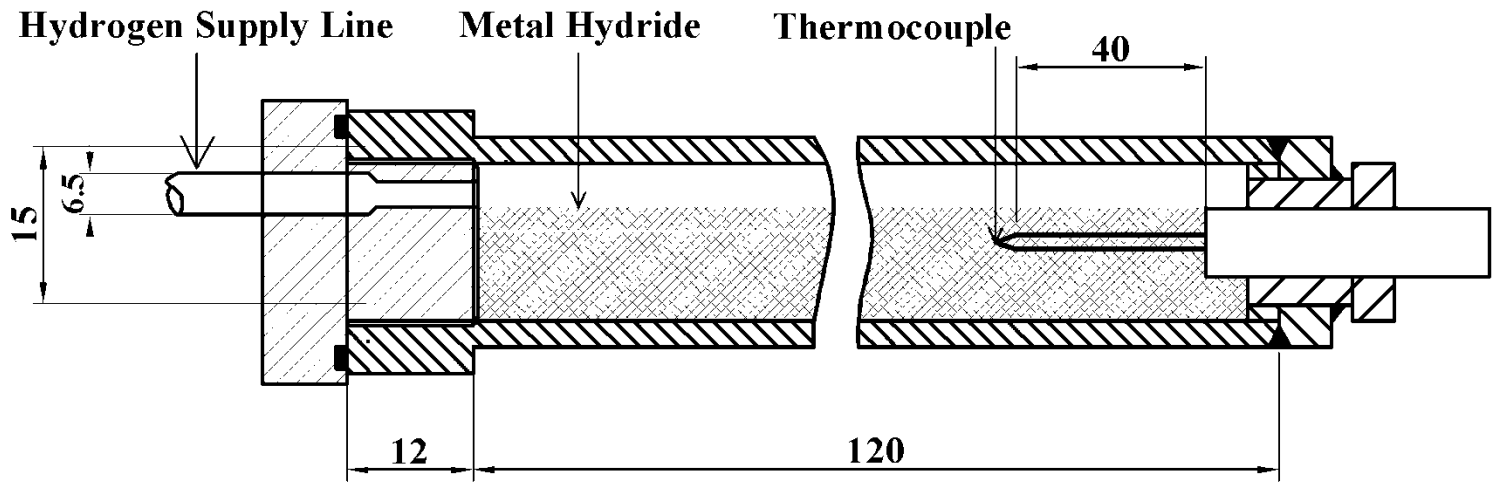

All the dimesions are in mm

Reactor for P-C-T measurements

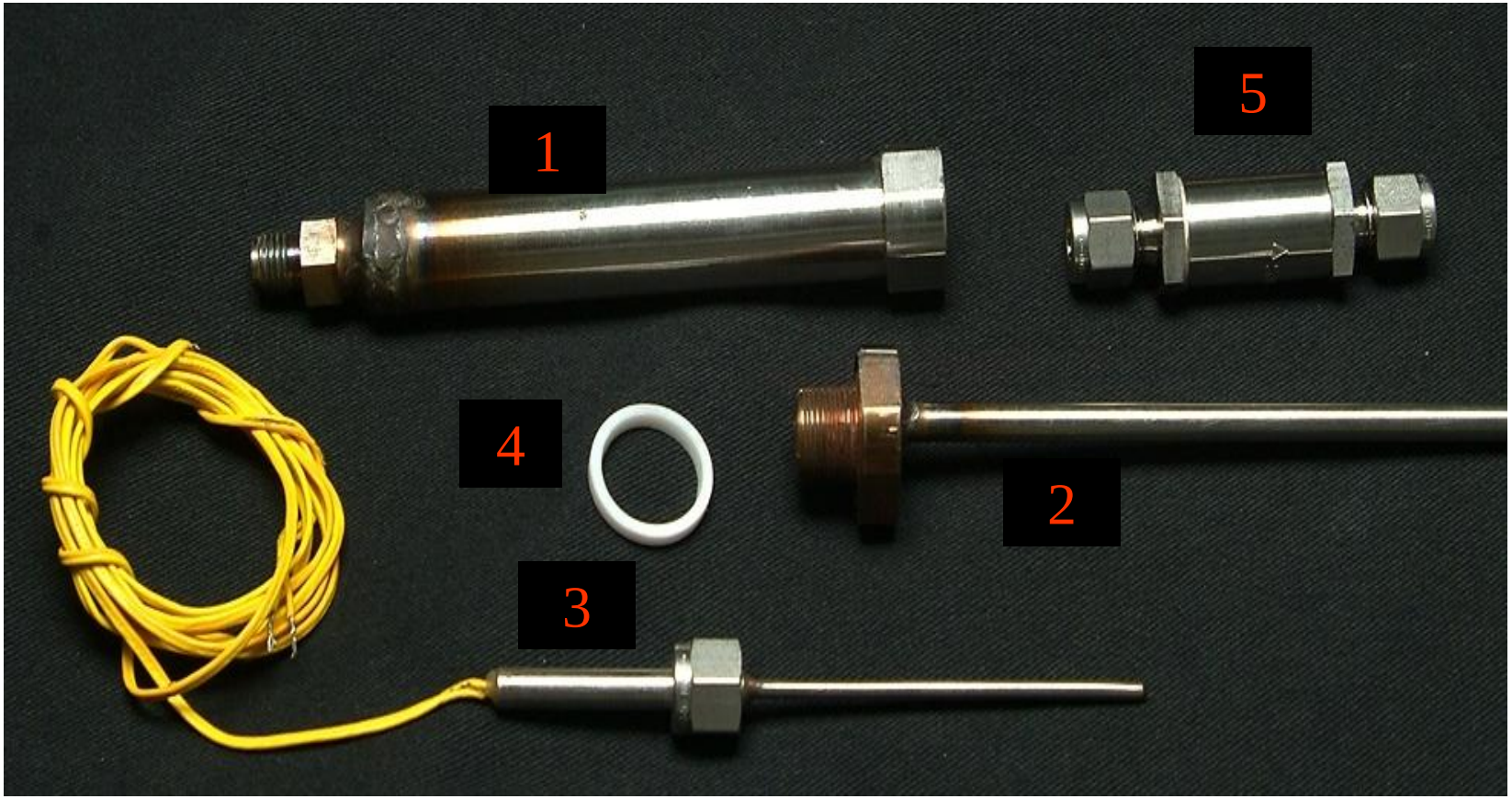

1.Reactor 2. Hydrogen Supply Line 3. Thermocouple
4.Teflon washer 5. In line Filter

Reactor parts

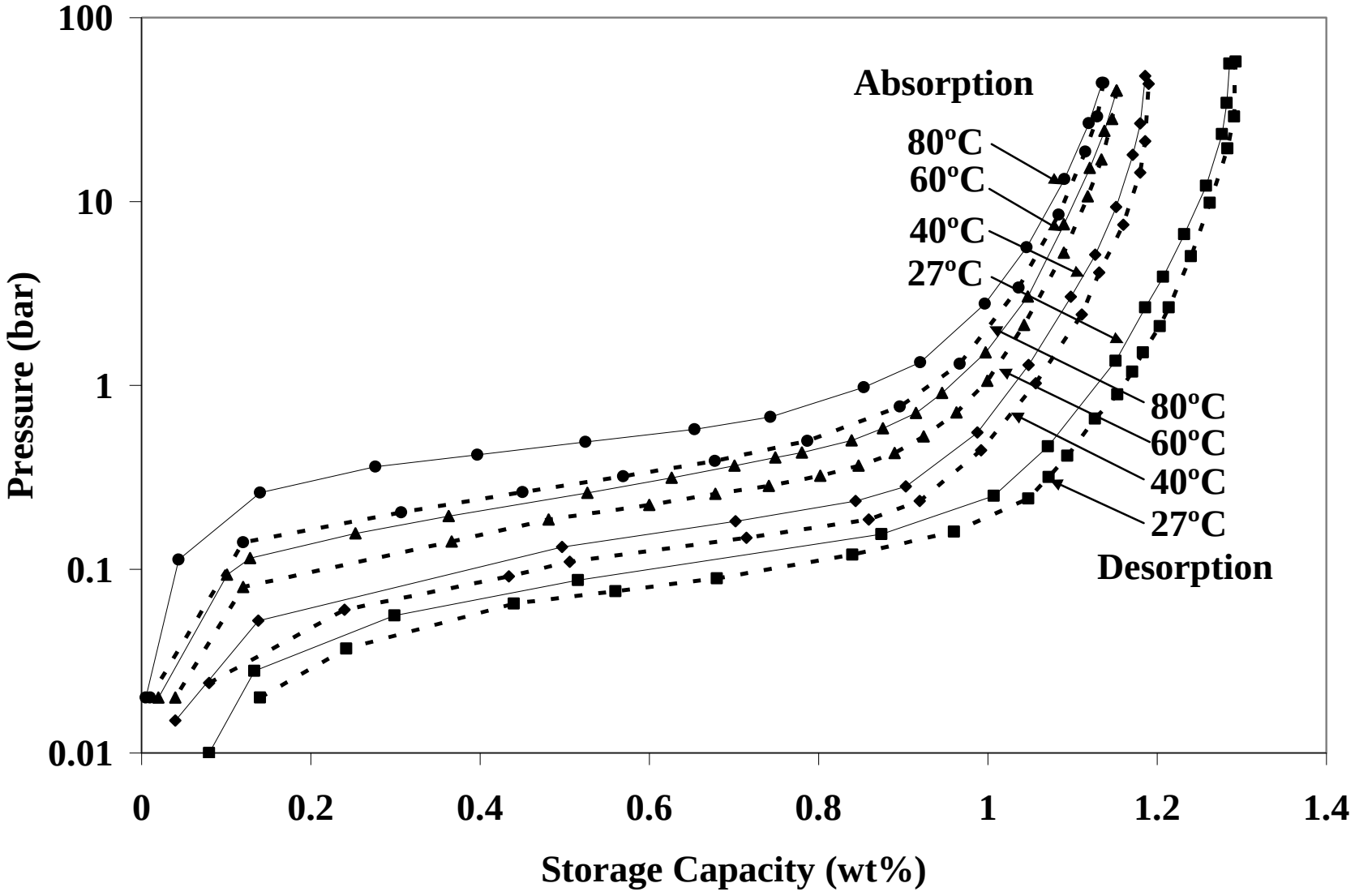

Static P-C-T characteristics for $MmNi_{3.9}Co_{0.5}Al_{0.6}$

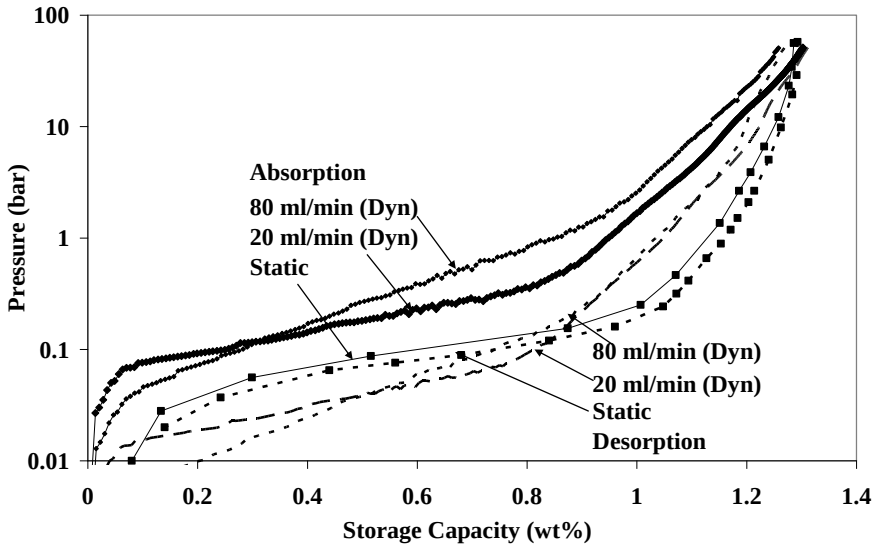

Comparison of static and dynamic P-C-T curves at 27ºC for $MmNi_{3.9}Co_{0.5}Al_{0.6}$

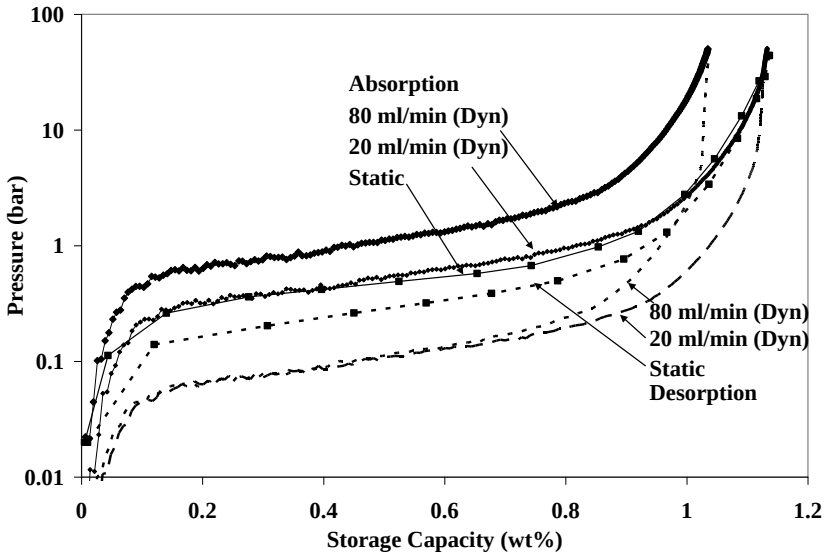

Comparison of static and dynamic P-C-T curves at 80ºC for $MmNi_{3.9}Co_{0.5}Al_{06}$

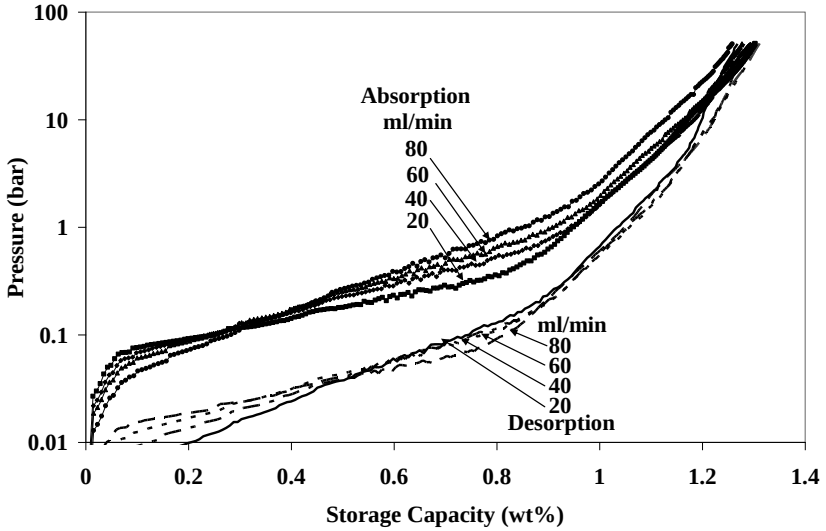

Effect of flow rate on plateau pressure at 27ºC for $MmNi_{3.9}Co_{0.5}Al_{0.6}$

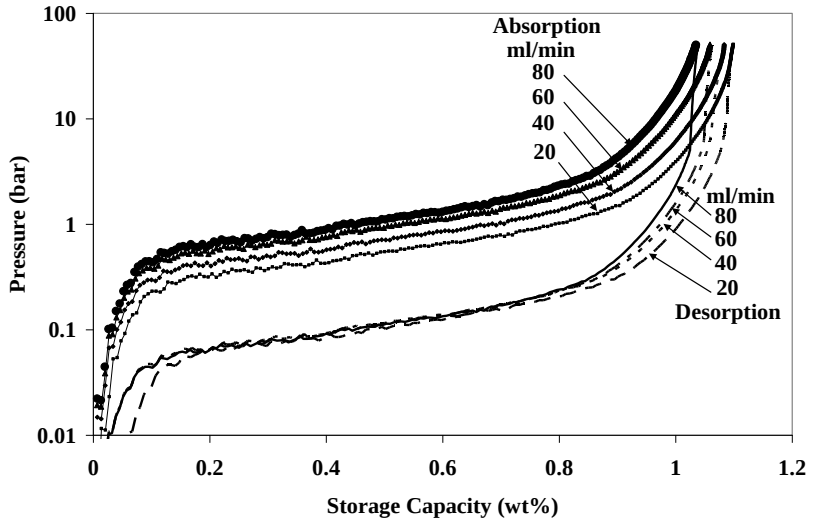

Effect of flow rate on plateau pressure at 80ºC for $MmNi_{3.9}Co_{0.5}Al_{0.6}$

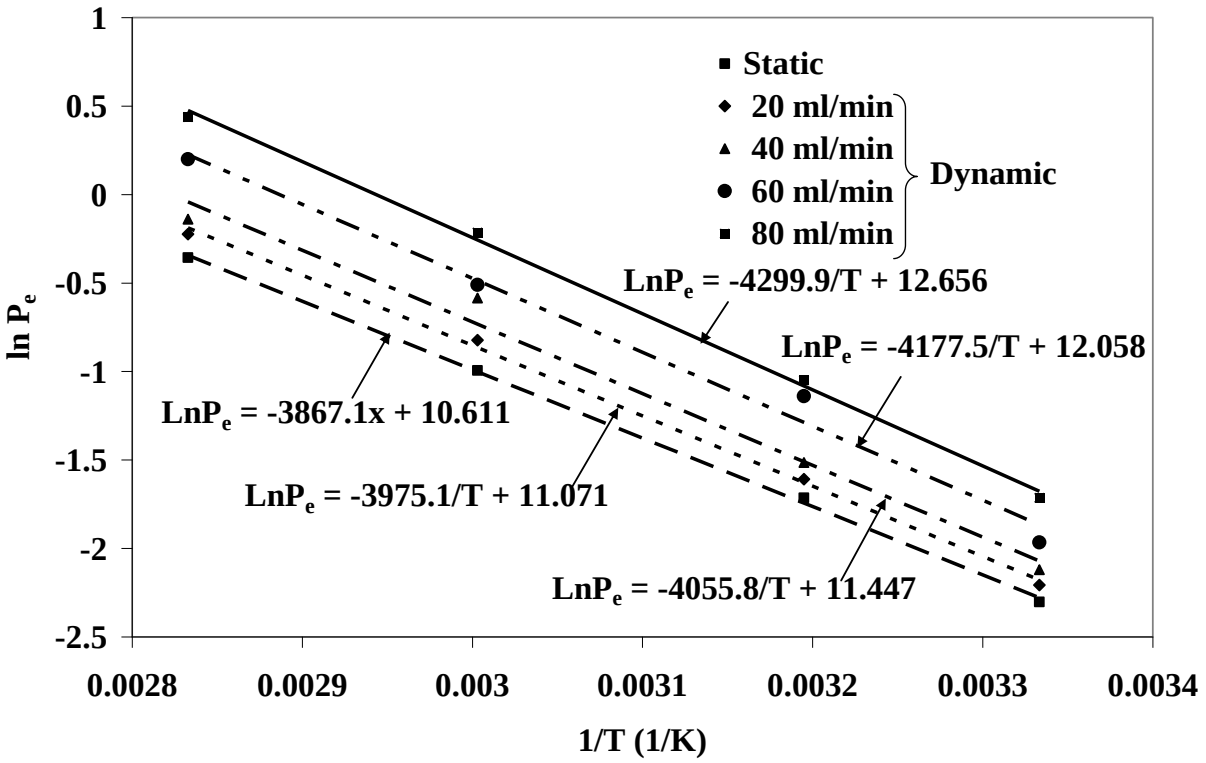

Ln(P_e) vs 1/T plots for $MmNi_{3.9}Co_{0.5}Al_{0.6}$

From van't Hoff equation

ΔH = 32.15 kJ/ g mol

ΔS= 0.088 kJ/ g mol K

S. No	Flow rate, ml/min	Apparent Enthalpy of formation, kJ/ g mol	Apparent Entropy of formation kJ/ g mol K
1	20	33.04	0.092
2	40	33.72	0.095
3	60	34.73	0.1
4	80	35.75	0.105

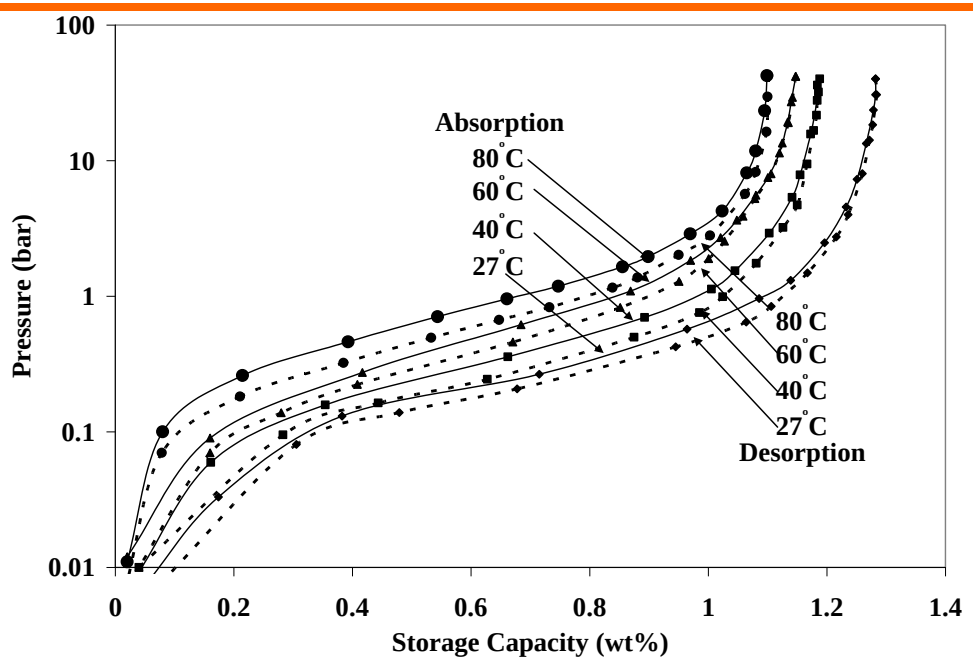

Static P-C-T characteristics for $MmNi_4Al$

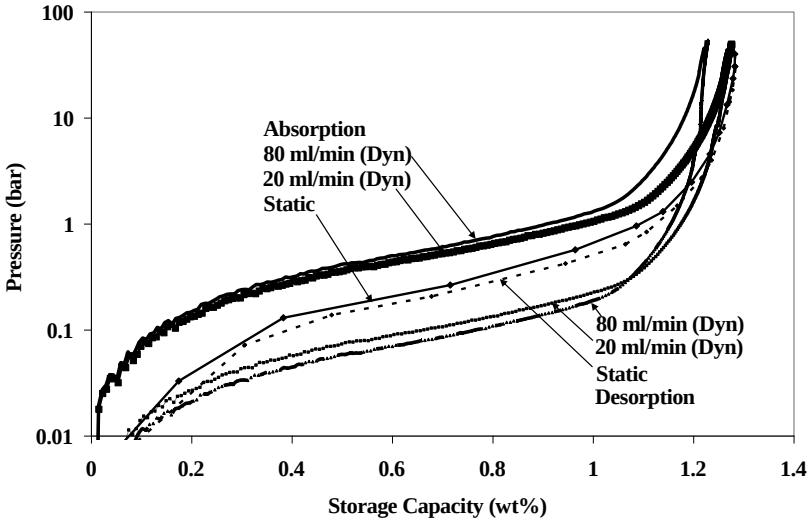

Comparison of static and dynamic P-C-T characteristics at 27ºC for $MmNi_4Al$

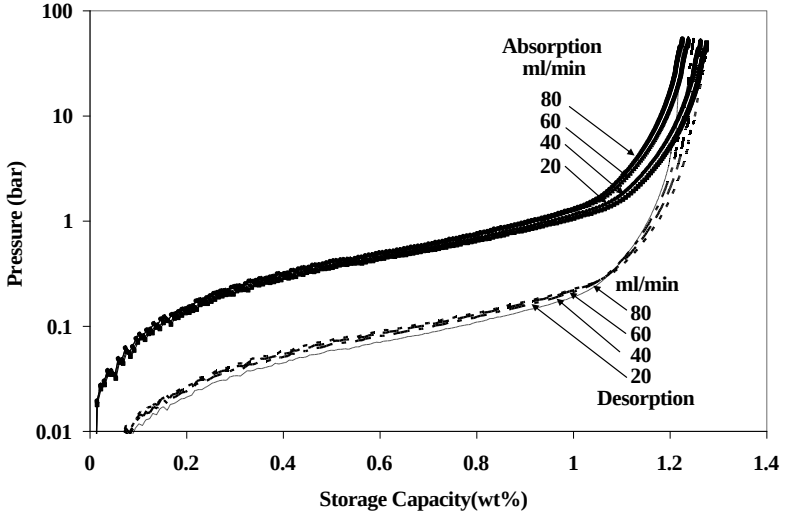

Effect of flow rate on plateau pressure at 27ºC for $MmNi_4Al$

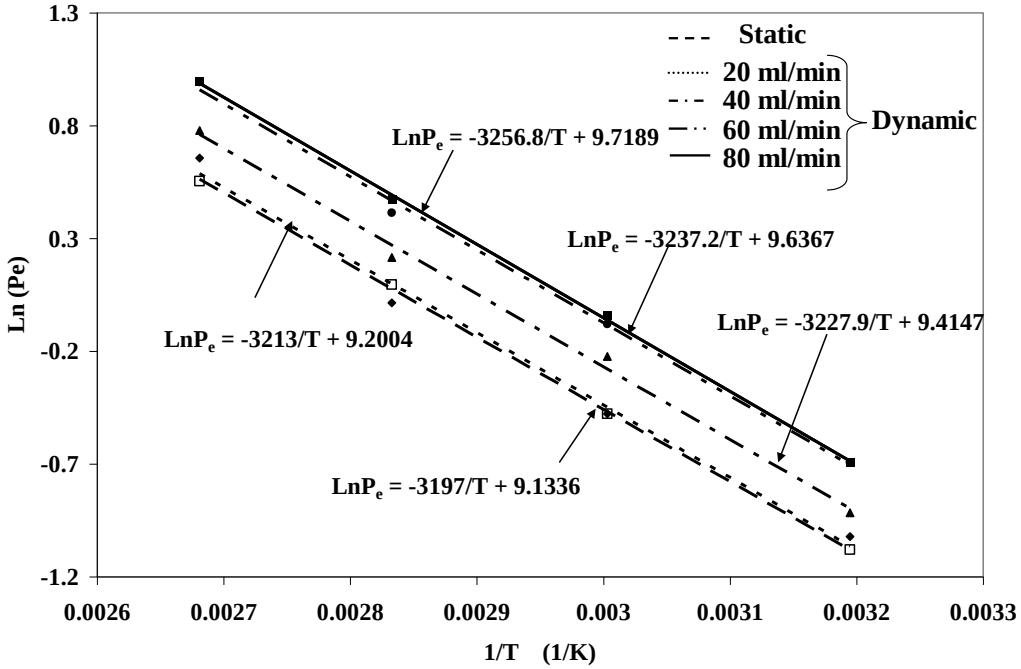

Ln(P_e) vs 1/T plots for $MmNi_4Al$

From van't Hoff equation

ΔH = 26.57 kJ/ g mol

ΔS= 0.076 kJ/ g mol K

S. No	Flow rate, ml/min	Apparent Enthalpy of formation, kJ/ g mol	Apparent Entropy of formation kJ/ g mol K
1	20	26.71	0.076
2	40	26.83	0.075
3	60	26.91	0.08
4	80	27.07	0.081

Comparison of thermodynamic properties for $MmNi_{5-x}Al_x$

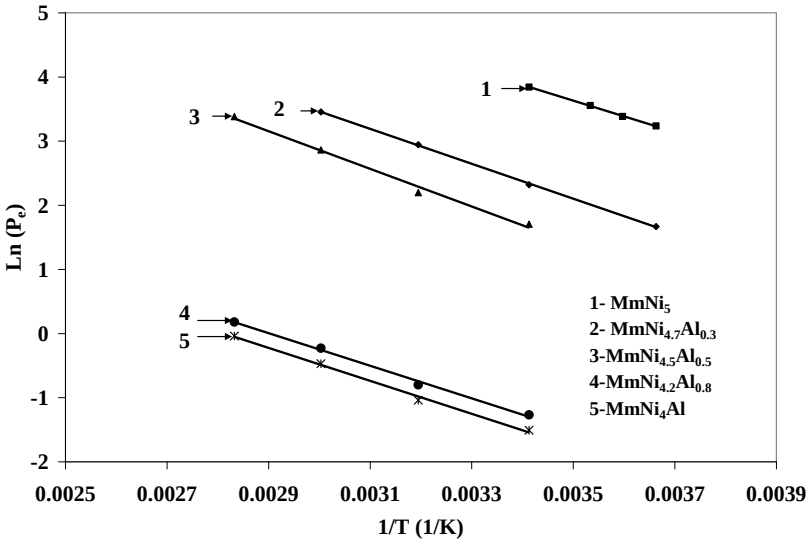

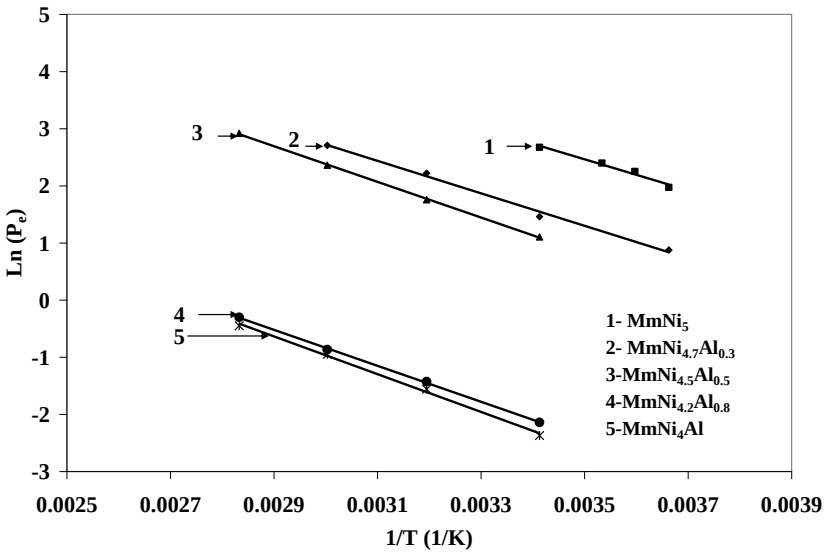

Composition	Enthalpy of formation at mid plateau, kJ/mol of H_2		Entropy of formation at mid plateau, kJ/mol of H_2 K		Difference in magnitude of Enthalpy of formation kJ/mol of H_2
	Absorption	Desorption	Absorption	Desorption	
$MmNi_5$	-20.356	22.548	-101.43	-99.41	2.192
$MmNi_{4.7}Al_{0.3}$	-22.629	24.286	-96.68	-93.51	1.657
$MmNi_{4.5}Al_{0.5}$	-24.417	25.966	-97.04	-95.43	1.548
$MmNi_{4.8}Al_{0.2}$	-25.091	26.579	-80.05	-75.93	1.488
$MmNi_4Al$	-26.175	27.486	-79.90	-82.757	1.31

Comparison of thermodynamic properties for multiple substituted alloys

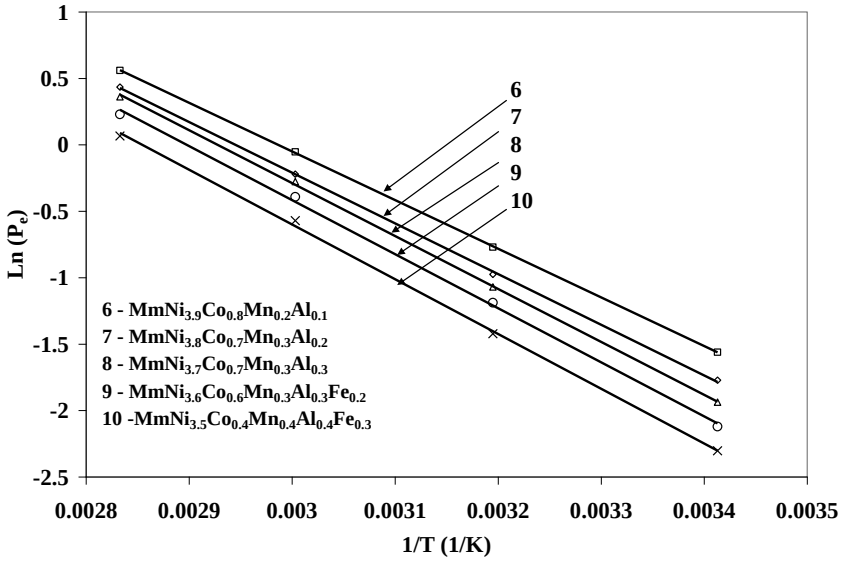

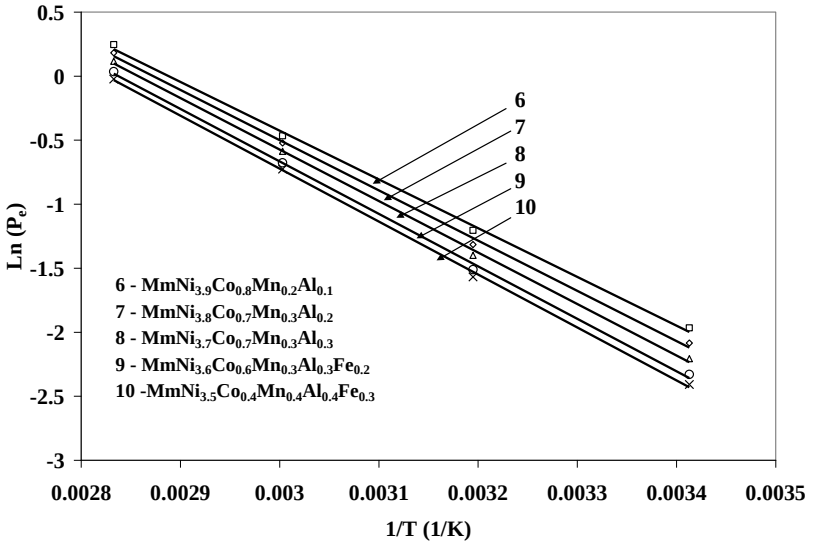

Composition	Enthalpy of formation at mid plateau, kJ/mol of H_2		Entropy of formation at mid plateau, kJ/mol of H_2 K		Difference in magnitude of Enthalpy of formation kJ/mol of H_2
	Absorption	Desorption	Absorption	Desorption	
$MmNi_{3.9}Co_{0.8}Mn_{0.2}Al_{0.1}$	-30.453	31.658	-90.94	-91.43	1.205
$MmNi_{3.8}Co_{0.7}Mn_{0.3}Al_{0.2}$	-31.709	32.609	-93.38	-93.67	0.9
$MmNi_{3.7}Co_{0.7}Mn_{0.3}Al_{0.3}$	-33.112	33.439	-96.94	-95.55	0.327
$MmNi_{3.6}Co_{0.6}Mn_{0.3}Al_{0.3}Fe_{0.2}$	-33.817	34.071	-97.98	-97.98	0.254
$MmNi_{3.5}Co_{0.4}Mn_{0.4}Al_{0.4}Fe_{0.3}$	-34.275	34.378	-97.83	-97.12	0.103

OBSERVATIONS

- There is no significant difference in the shapes of P-C-T curves and maximum hydrogen capacity between static and dynamic P-C-T measurements. However, hysteresis is larger in the case of dynamic P-C-T.
- The dynamic P-C-T depends on hydrogen flow rate. The effect of flow rate is less for the material with faster kinetics.
- Slope of Ln P_e vs 1/T curve increases from static to dynamic and it further increase with flow rate in dynamic P-C-T measurements
- Substitution of Al for Ni in $MmNi_5$ decreases the plateau pressure to subatmospheric values with marginal decrease in storage capacity and increase in plateau slope factor.
- The slope of van't Hoff lines increases with increase in Al content thereby increasing the enthalpy of reaction while the change in entropy is not significant.
- Hysteresis decreases with Al and multiple substitutions.

SORPTION KINETICS MEASUREMENTS

Kinetics is an important aspect in the design of the solid state storage device.

The kinetics (rate) equation in its simplest form is:

$$\dot{m} = -C_a \exp\left(-\frac{E_a}{RT}\right) \ln\left(\frac{P}{P_{eq}}\right)(\rho_{sat} - \rho_s)$$

A variety of models suggested as the sorption mechanism is a varying combination of physi- and chemi-sorption involving hydrogen in both molecular and atomic states.

In addition to the intrinsic material properties, its physical condition and production technique can have significant influence. Operating temperatures and pressures also can have good influence.

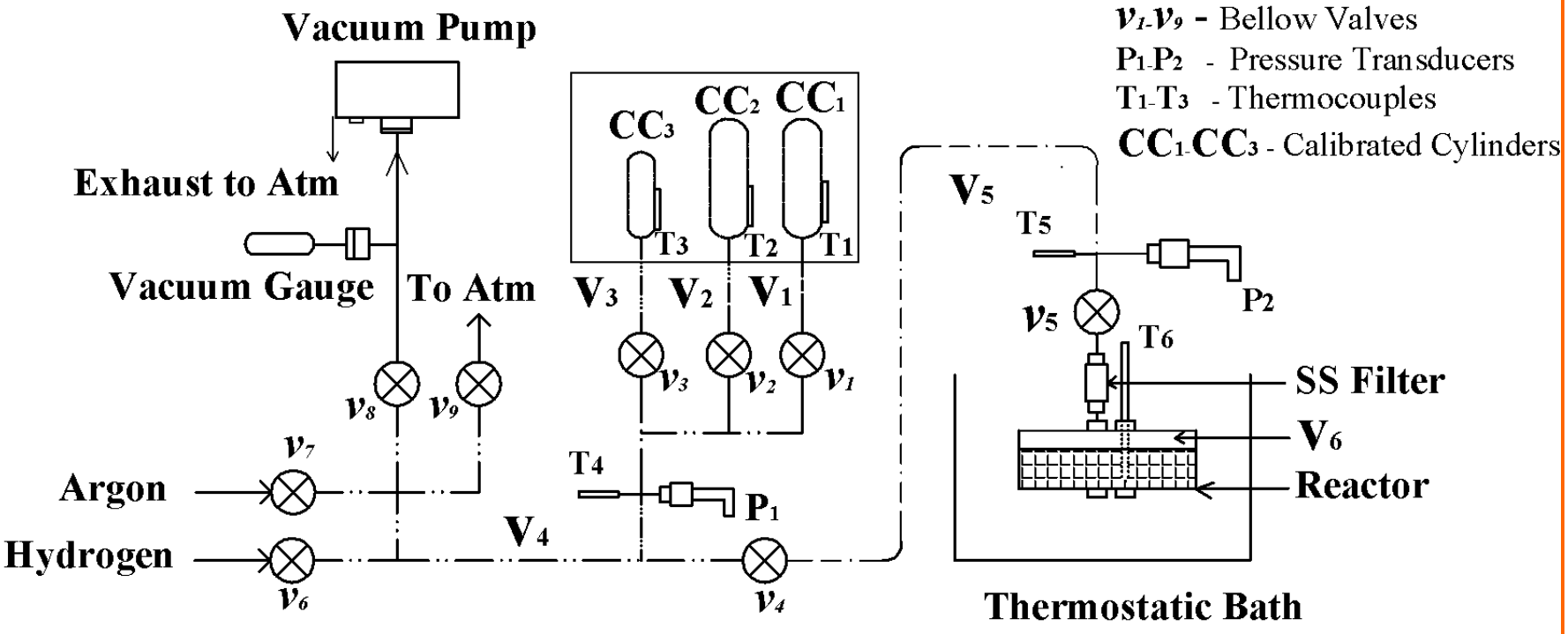

—·— V_1, Volume of CC_1 and pipe connecting CC_1 to v_1

—··— V_2, Volume of CC_2 and pipe connecting CC_2 to v_2

—···— V_3, Volume of CC_3 and pipe connecting CC_3 to v_3

—·· V_4, Volume of pipe between $v_1, v_2, v_3, v_4, v_6, v_7, v_8$ and v_9

— — · V_5, Volume of pipe between v_4 and v_5

——— V_6, Volume of free space in the reactor and pipe volume upto v_5

Schematic of experimental setup for kinetics measurements

Kinetics measurement calculations

Masses of hydrogen in V_1, V_2, V_3 and V_4 at the start of experiment

$$m_{i,s} = \frac{P_{i,s} V_i}{Z(P_{i,s}, T_{i,s}) R\, T_{i,s}}$$ **For i = 1 to 4**

Total mass of hydrogen at the start of experiment

$$m_s = \sum m_{i,s}$$ **For i = 1 to 4**

At any time t, masses of hydrogen in volumes V_1 to V_6 are calculated as follows

$$m_{i,t} = \frac{P_{i,t} V_i}{Z(P_{i,t}, T_{i,t}) R T_{i,t}}$$ **For i = 1 to 6**

Total mass of hydrogen in the system at time t is

$$m_t = \sum m_{i,t}$$ **For i = 1 to 6**

Mass of hydrogen absorbed till any particular time t is calculated as

$$m_{a,t} = m_s - m_t$$

Storage capacity (wt%) of hydrogen is calculated as

$$wt_t\% = \frac{m_{a,t}}{m_{alloy}} \times 100$$

Fraction absorbed is calculated as

$$\text{Fraction absorbed} = \frac{wt_t\%}{wt_T\%}$$

Kinetics measurement calculations

Masses in the volumes are calculated by

$$pV = Z(p,T)m_{H_2}R_{H_2}T$$

Where $Z(p,T)$ compressibility factor

For 280K ≤ T ≤ 428K

$$Z(p,T) = 1 + \left(B_0 + B_1T + B_2T^2\right)p + \left(C_0 + C_1T + C_2T^2\right)p^2$$

For 428K ≤ T ≤ 800K

$$Z(p,T) = 1 + \left(B_0 + B_1T + B_2T^2\right)p$$

$B_0 = 0.009662\ MPa^{-1}$
$B_1 = -1.5446 \times 10^{-5}\ MPa^{-1}K^{-1}$
$B_2 = 8.2314 \times 10^{-9}\ MPa^{-1}K^{-2}$

$C_0 = 1.8167 \times 10^{-4}\ MPa^{-2}$
$C_1 = -8.3222 \times 10^{-7}\ MPa^{-2}K^{-1}$
$C_2 = 9.527 \times 10^{-10}\ MPa^{-2}K^{-2}$

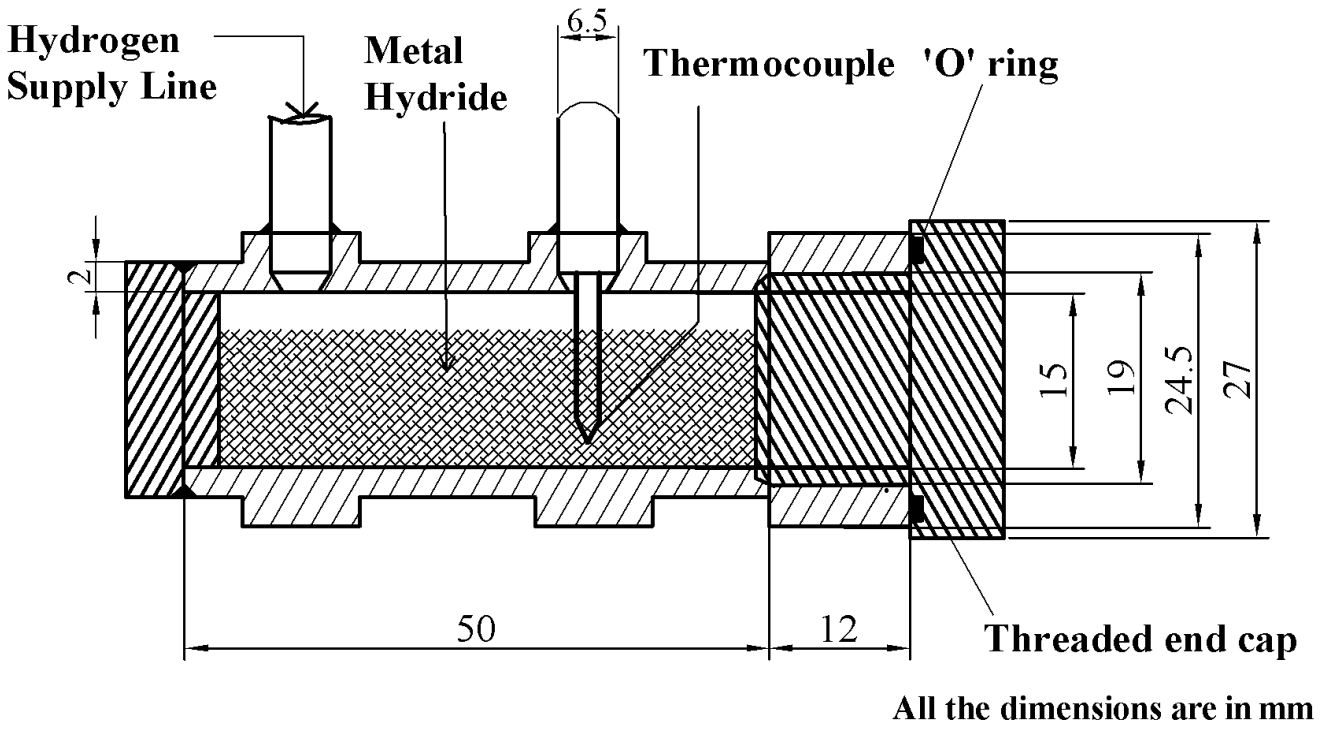

Reactor for kinetics measurements

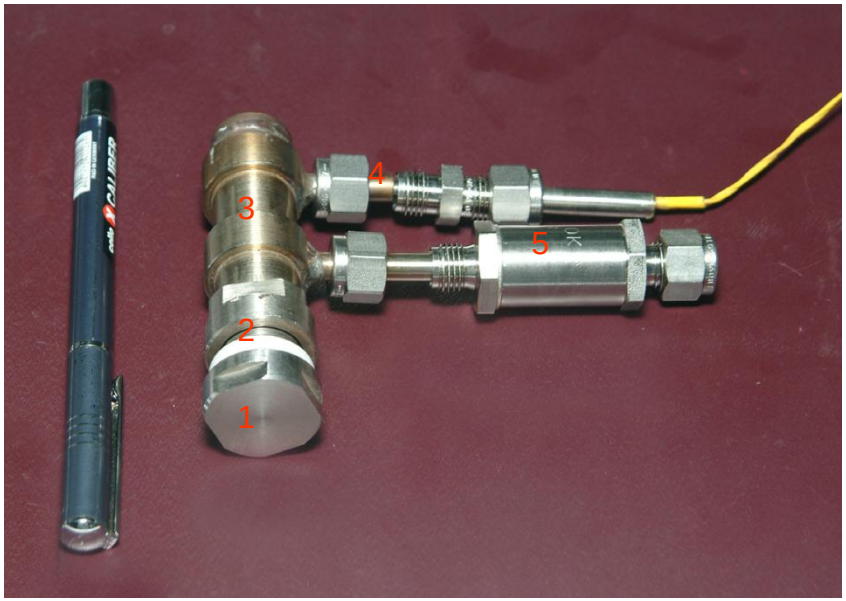

1. End Cap 2. Teflon Washer 3.SS-Tube 4. Thermo couple 5. SS Filter

Reactor for kinetics measurements

The Johnson-Mehl-Avrami(JMA) equation

$$\alpha(t) = 1 - \exp[-(kt)^n]$$

Where α(t) is the absorbed fraction at any time t, k is the rate constant and η is the Avarami constant.

The above equation can be rewritten as

$$\log[-\ln(1-\alpha)] = \eta \log t + \eta \log k$$

Arrhenius equation

$$k = k_0 \exp\left(\frac{-E_A}{\mathrm{RT}}\right)$$

Which can be rewritten as

$$\ln k = -\frac{E_A}{RT} + \ln k_o$$

η<1	**Surface controlled growth**
1<η<1.5	**Growth of nuclei beyond a critical volume**
η=1.5	**Growth of nuclei with a nucleation rate close to zero**
1.5< η<2.5	**Growth of nuclei with decreasing nucleation rate**
η=2.5	**Growth of nuclei with constant nucleation rate**
η>2.5	**Growth of small nuclei with an increasing nucleation rate**

Modified JMA plots

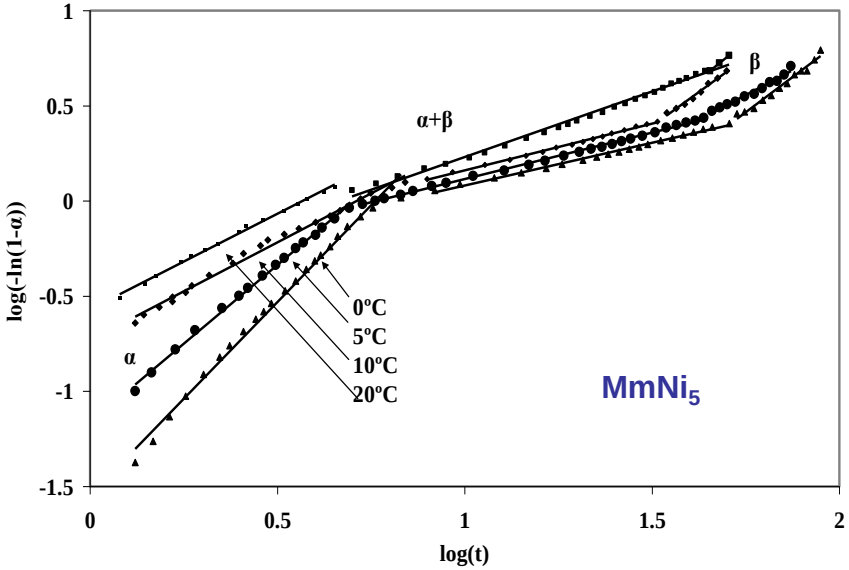

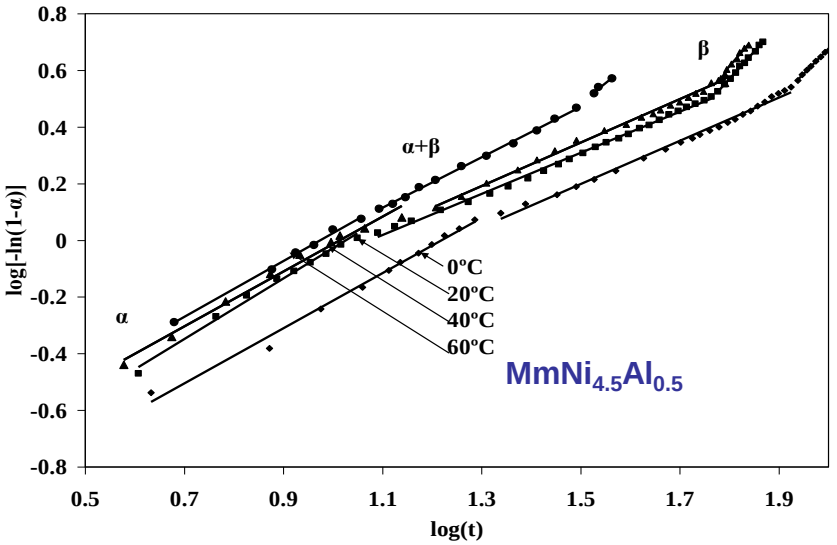

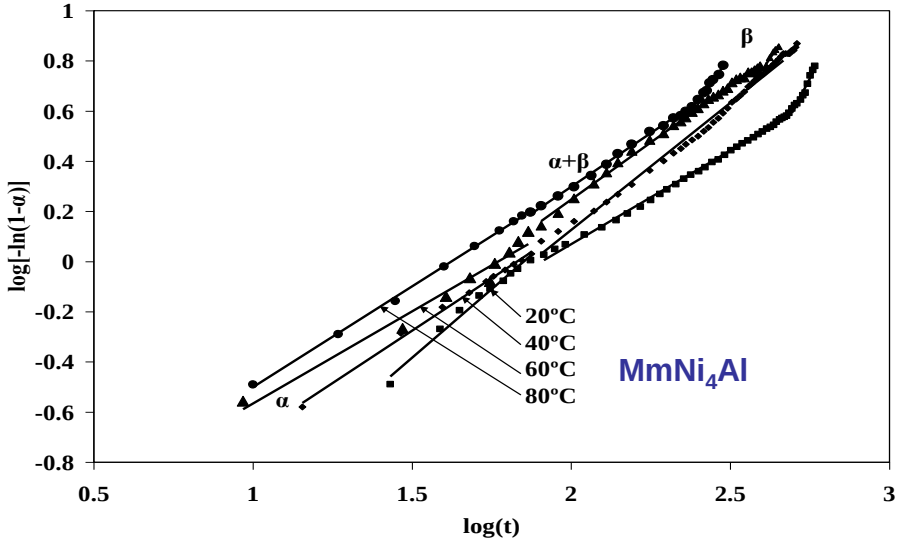

Rate constants and Avarami constants

Material	Temperature, °C	Surface Process (α phase)		Interface Process (α-β phase)	
		Rate constant, s^{-1}	η	Rate constant, s^{-1}	η
$MmNi_5$	0	0.194296	1.0289	0.14774	0.4906
	5	0.209876	1.6566	0.171816	0.4871
	10	0.233634	1.0714	0.172045	0.4504
	20	0.2755	1.0761	0.216794	0.6877
$MmNi_{4.5}Al_{0.5}$	0	0.028043	1.0706	0.024502	0.7455
	20	0.061582	1.128	0.047549	0.8276
	40	0.112478	1.2613	0.093344	0.7288
	60	0.19398	1.4459	0.146168	0.8581
$MmNi_4Al$	20	0.004942	1.0939	0.004663	0.7455
	40	0.014806	1.1154	0.013302	0.8118
	60	0.0117	1.2613	0.026226	0.7288
	80	0.06081	1.4023	0.052392	0.8556

Arrehenius plots and Activation energies

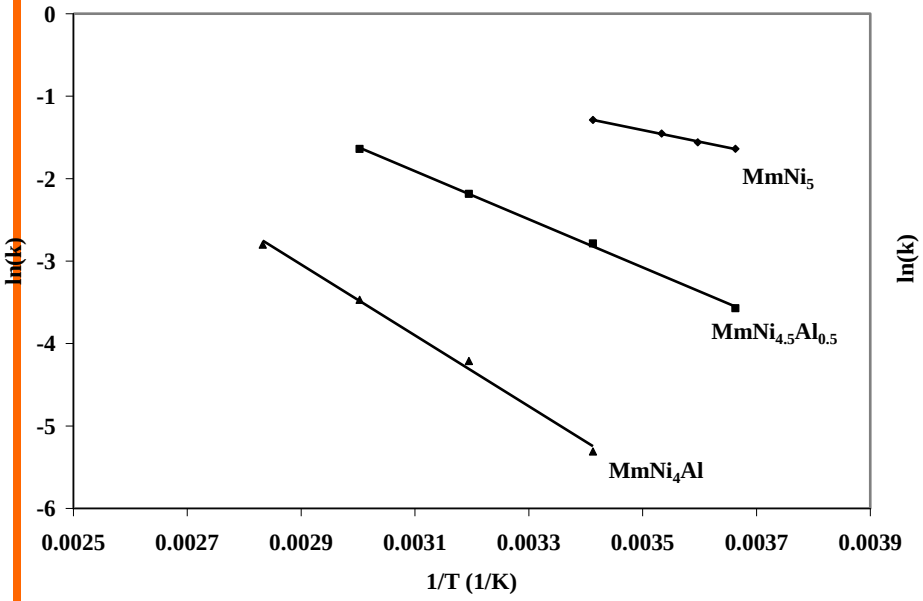

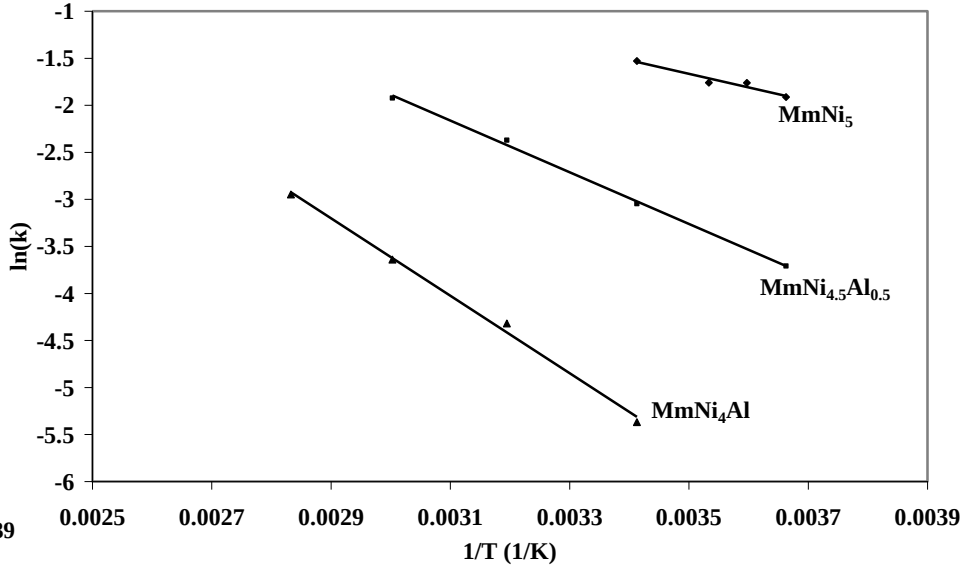

Material	Apparent activation Energies kJ/mol K	
	α	α+β
$MmNi_5$	15.061	15.019
$MmNi_{4.5}Al_{0.5}$	24.261	22.841
$MmNi_4Al$	35.716	34.235

MEASUREMENT OF EFFECTIVE THERMAL CONDUCTIVITY OF METAL HYDRIDE BEDS

The knowledge of effective thermal conductivity of metal hydride bed and its dependence on hydrogen pressure and concentration and bed temperature is essential for successful design of metal hydride reactor.

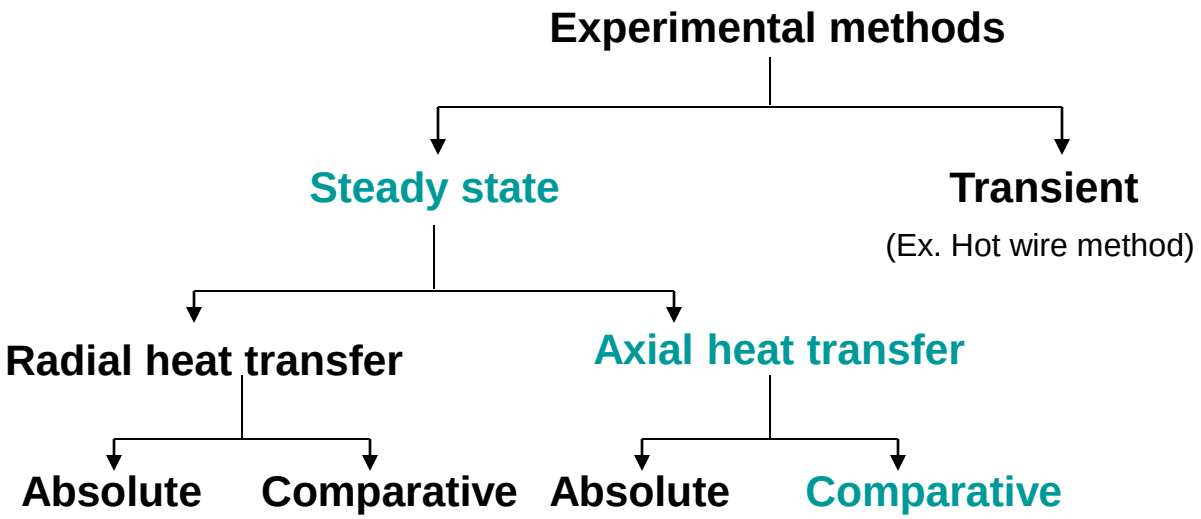

As in the case of packed beds, effective thermal conductivity (k_e) of metal hydride beds also depends on parameters like packing density, bed porosity, particle size, etc.

Additionally, porosity of the solid particle, sorbed hydrogen concentration, hydrogen pressure also play an important role.

During the charging and discharging of the storage device, k_e changes due to changes in hydrogen concentration and expansion of the particles.

These are difficult to predict, and measured data on these are rather scarce.

Effective thermal conductivity of metal hydride beds

S.No	Material	Operating variables		k_e Value W/m K	Testing method	Reference
		Pressure bar	Temperature K			
01.	**$TiMn_{1.5}$**	0.1 to 50		**0.2 to 1.2**	Steady, radial, comparative	Suda et al (1980)
02.	**$TiFeH_x$**	--	298	**1.49**	Transient temperature measurement	Godell P.D. (1980)
03.	**$LaNi_5H_x$**	--	298	**1.32**	Transient temperature measurement	Godell P.D. (1980)
04.	**$MgH_{1.8}$**	40	313	**1.3**	Transient hot wire	Ishido et al (1982)
05.	**Mg_2NiH_4**	45	373	**0.8**	Transient hot wire	Ishido et al (1982)
06.	**Mg_2NiH_4**	45	373	**0.83**	Steady, radial, comparative	Suissa et al (1984)
08.	**$MmNi_4FeH_{5.2}$**	45	273	**1.05**	Steady, radial , comparative	Suissa et al (1984)
09.	**$TiFe_{0.85}Mn_{0.15}$**	10^{-8} to 55	273 to 423	**0.1 to 1.5**	Steady, axial, absolute	Kempf and Martin (1986)
10	**$MlNi_{4.5}Mn_{0.5}H_x$**	30	300	**1.3**	Steady, radial , comparative	Da-Wen Sun (1990)
11	**$LaNi_5$**	0.01 to 10	---	**0.1 to 1.5**	Transient, 2D, Identification technique	Pons and Dantzer (1994)
12	**$LaNi_{4.7}Al_{0.3}H_x$**	10^{-6} to 60	193 to 413	**0.02 to1.2**	Transient hot wire	Hahne and Kallweit (1998)
13	**$Ti_{0.98}Zr_{0.02}V_{0.43}Fe_{0.09}Cr_{0.05}Mn_{1.5}H_x$**	10^{-6} to 60	193 to 413	**0.05 to 1.2**	Transient hot wire	Hahne and Kallweit (1998)
14	**Mg and 2% Ni**	0.1 to 50	573 to 673	**4 to 9**	Transient radial	Kapischke and Hapke (1994)
15	**$Mg\text{-}MgH_2$**	0.1 to 50	523 to 653	**2 to 8**	Oscillating heating technique	Kapischke and Hapke (1998)

Effective thermal conductivity measurement cell

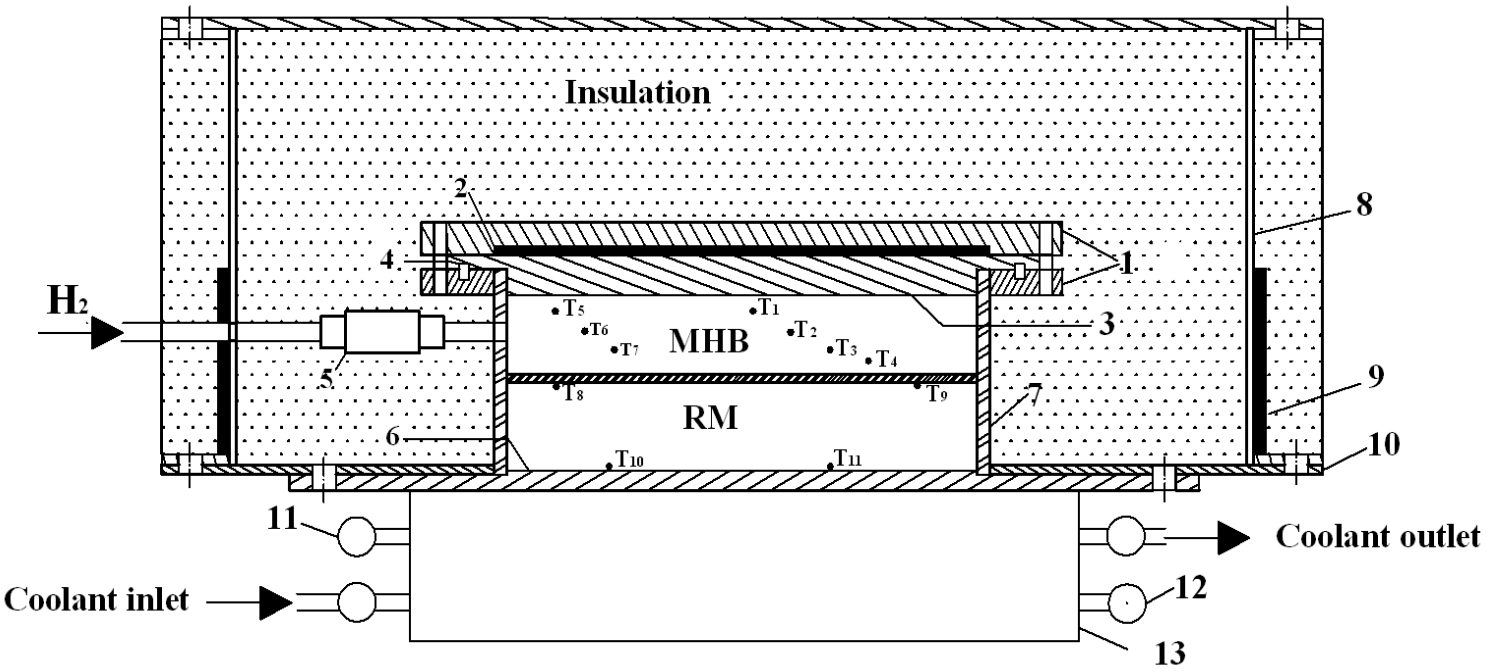

1 - Top end flanges 2 - Main heater 3 - Hot plate 4 - PTFE washer 5 - SS Filter 6 - Cold plate

7 - Metal hydride bed and reference material container (SS316 tube) 8 - Outer container 9 - Guarded heater

10 - Bottom end flange 11 and 12 - Top and bottom ring shaped coolant distributors 13 - Cooling chamber

MHB - Metal hydride bed RM - Reference material • Thermocouples ($T_{1....11}$)

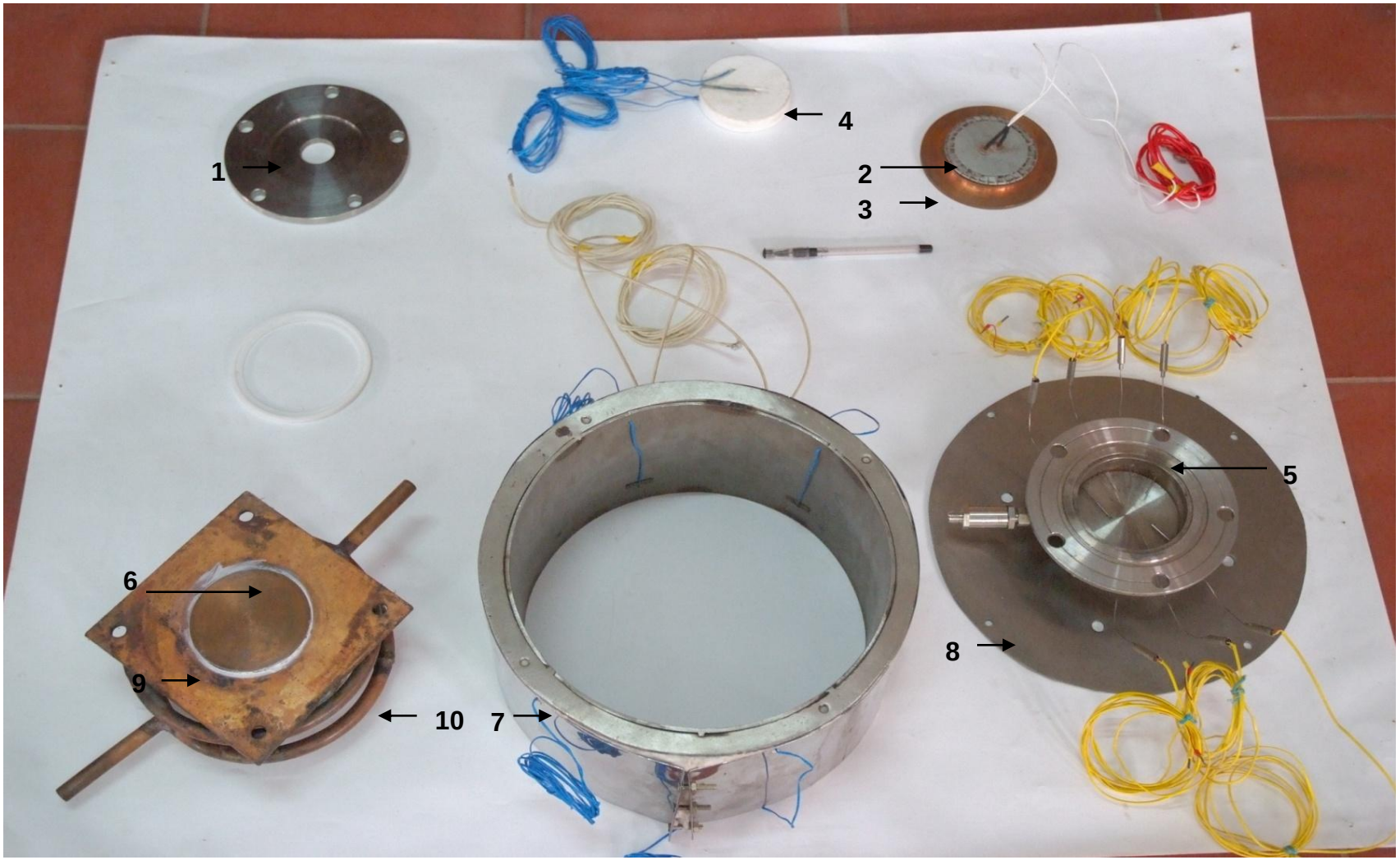

1.Top flange 2. Main heater 3. Hot plate 4. PTFE washer 5. Top lower flange

6. Cold plate 7. Guarded heater 8. Bottom flange 9. Top copper ring 10. Bottom copper ring

Parts of effective thermal conductivity measurement cell

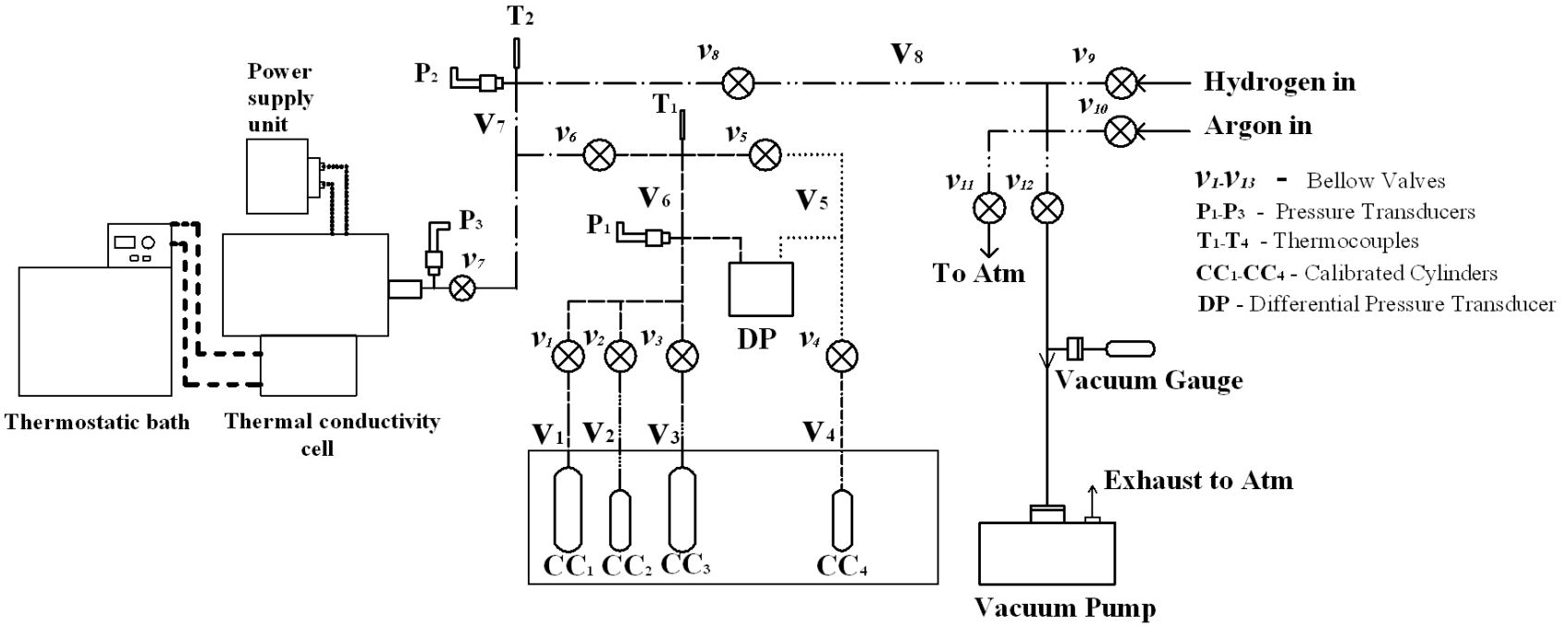

V_1, Volume of CC_1 and pipe connecting CC_1 to v_1

V_2, Volume of CC_2 and pipe connecting CC_2 to v_2

V_3, Volume of CC_3 and pipe connecting CC_3 to v_3

V_4, Volume of CC_4 and pipe connecting CC_4 to v_4

V_5, Volume of pipe between v_4, v_5 and DP

V_6, Volume of pipe between v_1, v_2, v_3, v_5, v_6 and DP

V_7, Volume of pipe between v_6, v_7 and v_8

V_8, Volume of pipe between v_8, v_9, v_{10}, v_{11} and v_{12}

Experimental setup for measuring effective thermal conductivity

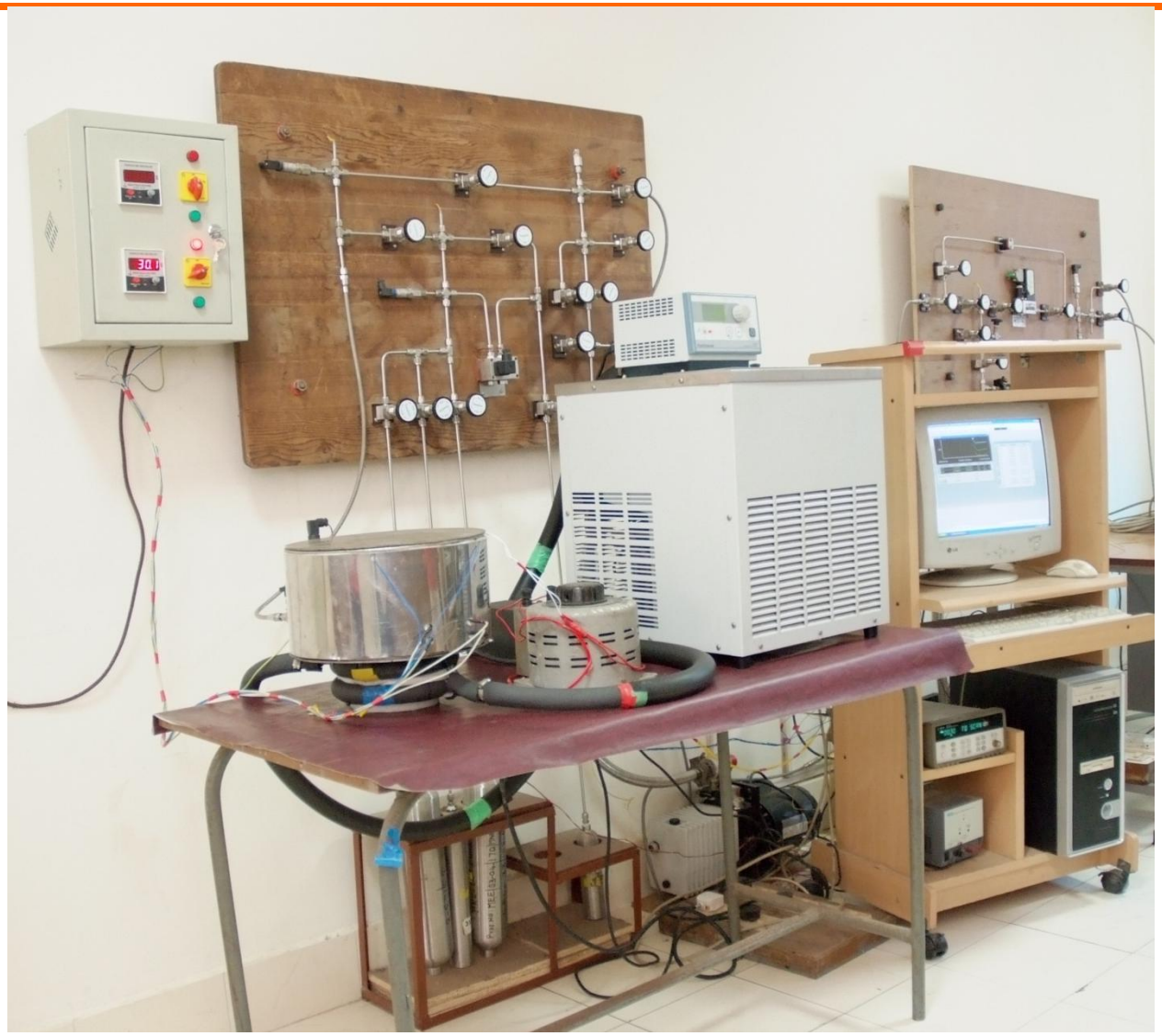

Experimental setup for measuring effective thermal conductivity

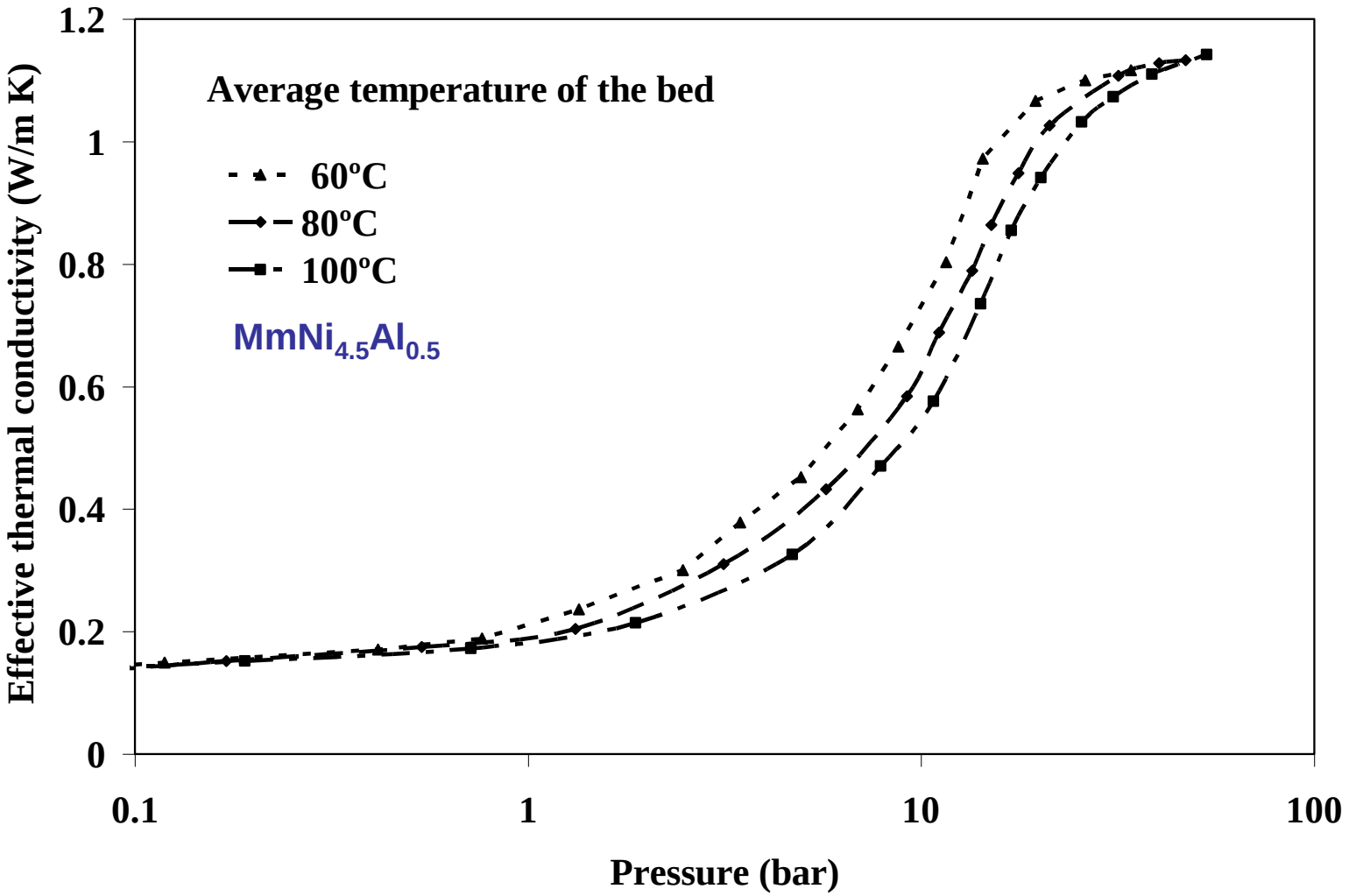

Variation of Effective thermal conductivity with pressure at different temperatures

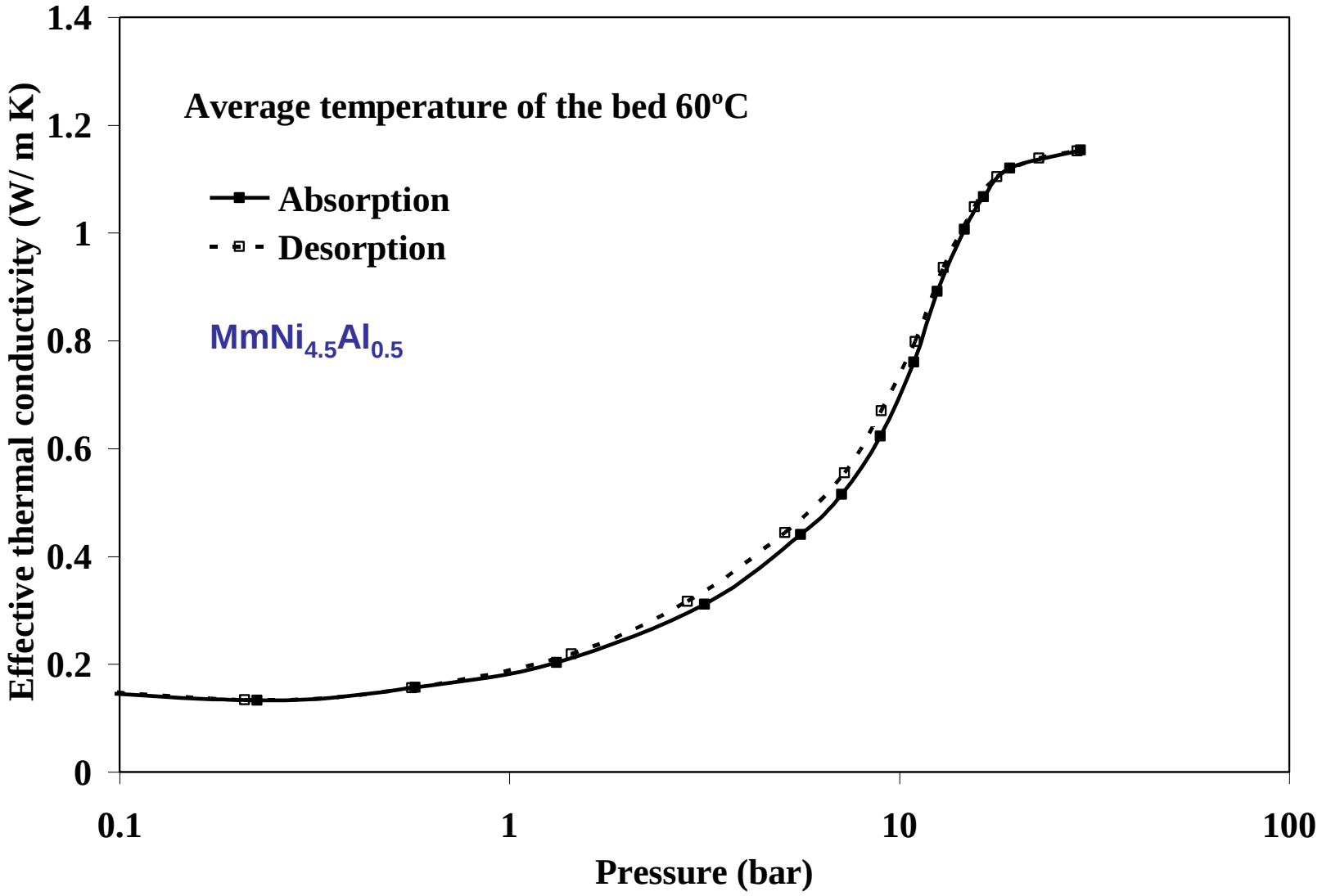

Variation of effective thermal conductivity with pressure during absorption and desorption

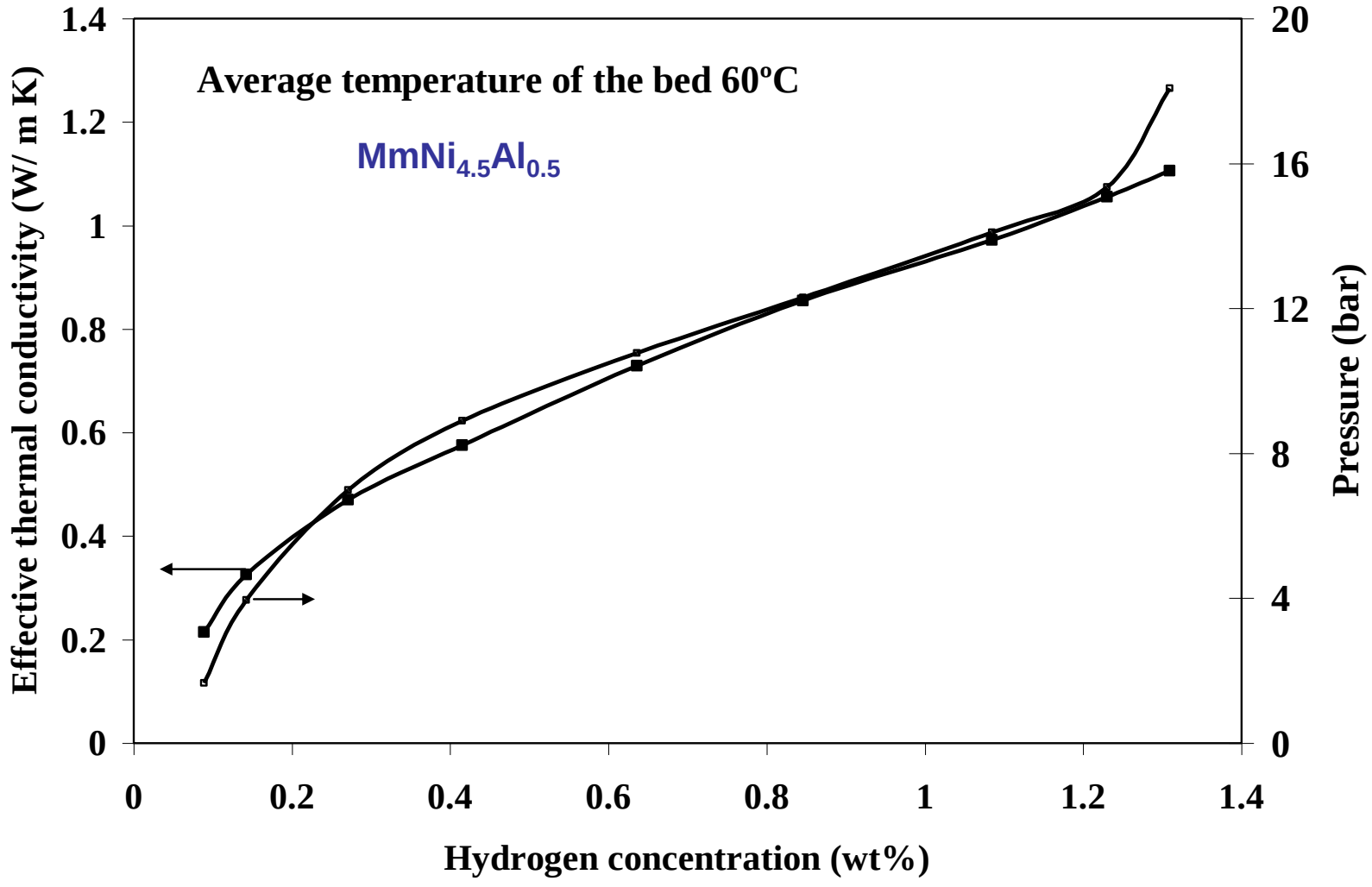

Variation of effective thermal conductivity with concentration during absorption

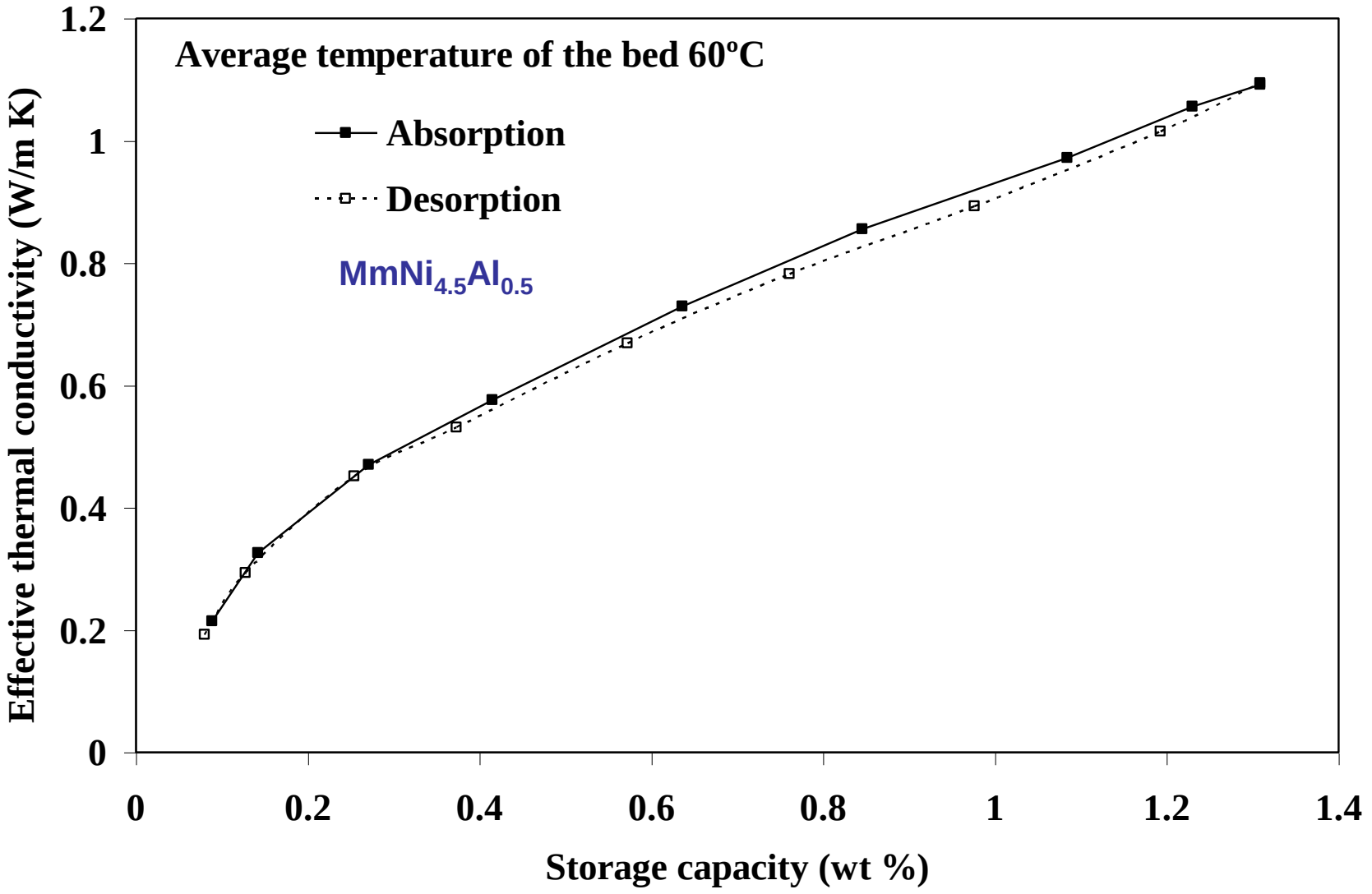

Variation of effective thermal conductivity with concentration during absorption and desorption

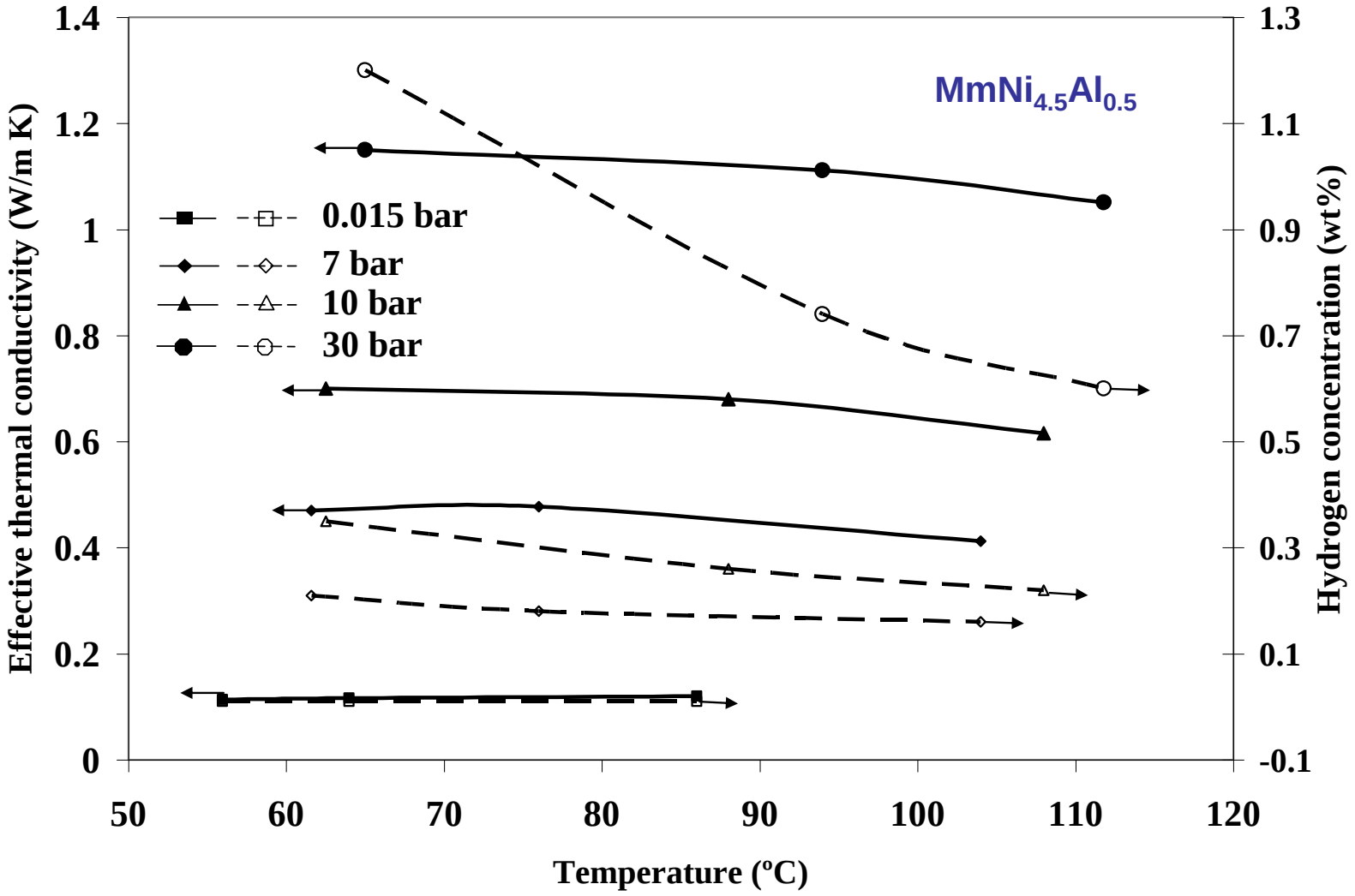

Variation of effective thermal conductivity with temperature at different pressures

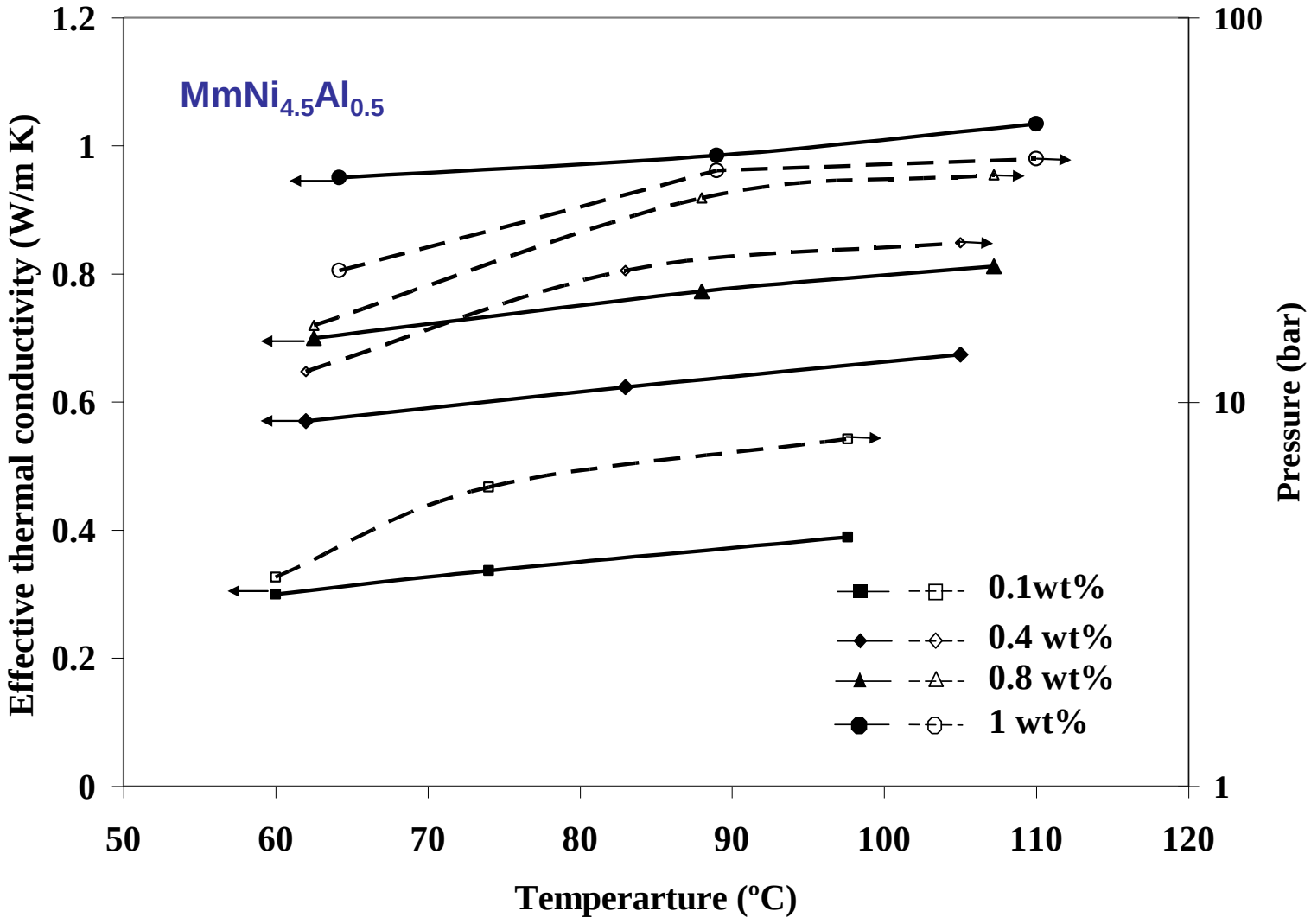

Variation of effective thermal conductivity with temperature at different concentrations

The experimental results are analysed using Yagi and Kunii theoretical model

In case of fine particles and motionless gas the effective thermal conductivity is given as

$$\frac{k_e}{k_g^*} = \beta \frac{1-\varepsilon}{\frac{k_g^*}{k_s^*} + \varphi}$$

Where

k_e is the effective thermal conductivity of metal hydride bed, W/ m K

k_g^* is effective thermal conductivity of gas, W/m K

k_s^* is effective thermal conductivity of solid, W/m K

ε is porosity of the bed

φ is Effective thickness of fluid in void in relation to the thermal conduction/mean diameter of the solid (l_v/D_p) empirically estimated as 0.078 in the porosity rage of 0.3 to 0.5

β is the ratio of the average length between the centers of two neighbouring solids in the direction of heat flow to the mean diameter of packing, is assumed to be unity.

The effective thermal conductivity of the gas in the pore is calculated using Chapman and Cowlings formula

$$\frac{k_g}{k_g^*} = 1 + \frac{2\sigma}{X_e}\left(\frac{2}{\gamma} - 1\right)$$

Where

k_g is the thermal conductivity of gas in infinite space, W/ m K

σ is mean free path of gas molecules, m

X_e is the effective pore length, m

γ accommodation coefficient, (taken as 0.15)

Particle diameter is calculated using experimentally measured break even pressure

$$P_b = 1770 \times 10^{-24} \frac{t}{s^2 D}$$

Where

P_b is break even pressure, N/m^2

t is temperature, ^{o}C

S hydrogen molecule diameter, m

D particle diameter

The mean free path is a function of density of the gas in pore in turn it is a function of pressure and temperature

$$\sigma = \frac{2.331 \times 10^{-20} \times T}{s^2 P}$$

Where

S is hydrogen molecular diameter, m

T is temperature, K

P is Pressure, N/m^2

σ is mean free path of gas molecules, m

Porosity of the bed is a function of concentration of hydrogen in the metal. Assuming linear variation of porosity with concentration it can be expressed as

$$\varepsilon = \varepsilon_o - (1-\varepsilon_o) \times (\mathrm{wt\%} / \mathrm{wt}_{max}\,\%) \times f_{VE}$$

Where

ε_o is the initial porosity of the bed (without hydrogen)

f_{VE} is the maximum expansion factor

Maximum expansion factor can be calculated as

$$f_{VE} = \frac{\Delta V \times N_A \times (H/M)_{max} \times \rho_s \times 2 \times 10^{-3}}{M_s \times M_{H_2}}$$

ΔV is volume expansion of the metal atom, 2.9×10^{-30} m^3/H-atom

N_A is Avogadro's constant, 6.0221415×10^{23}

ρ_s is alloy density, kg/m^3

H/M_{max} is weight of hydrogen absorbed per mol of metal, g of H_2/mol metal

M_s is molecular weight of alloy

M_{H2} is molecular weight of hydrogen

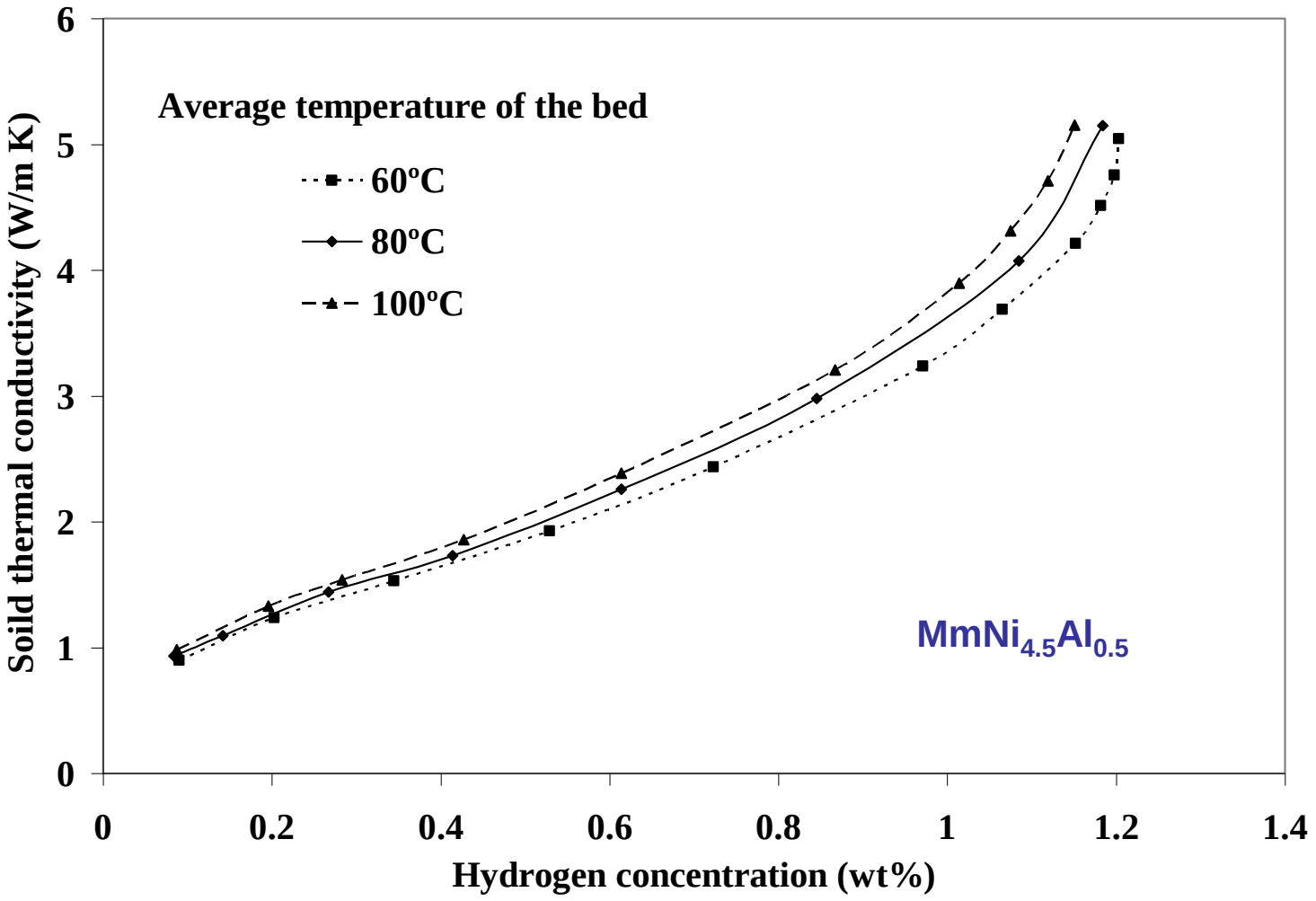

Variation of effective solid thermal conductivity with hydrogen concentration

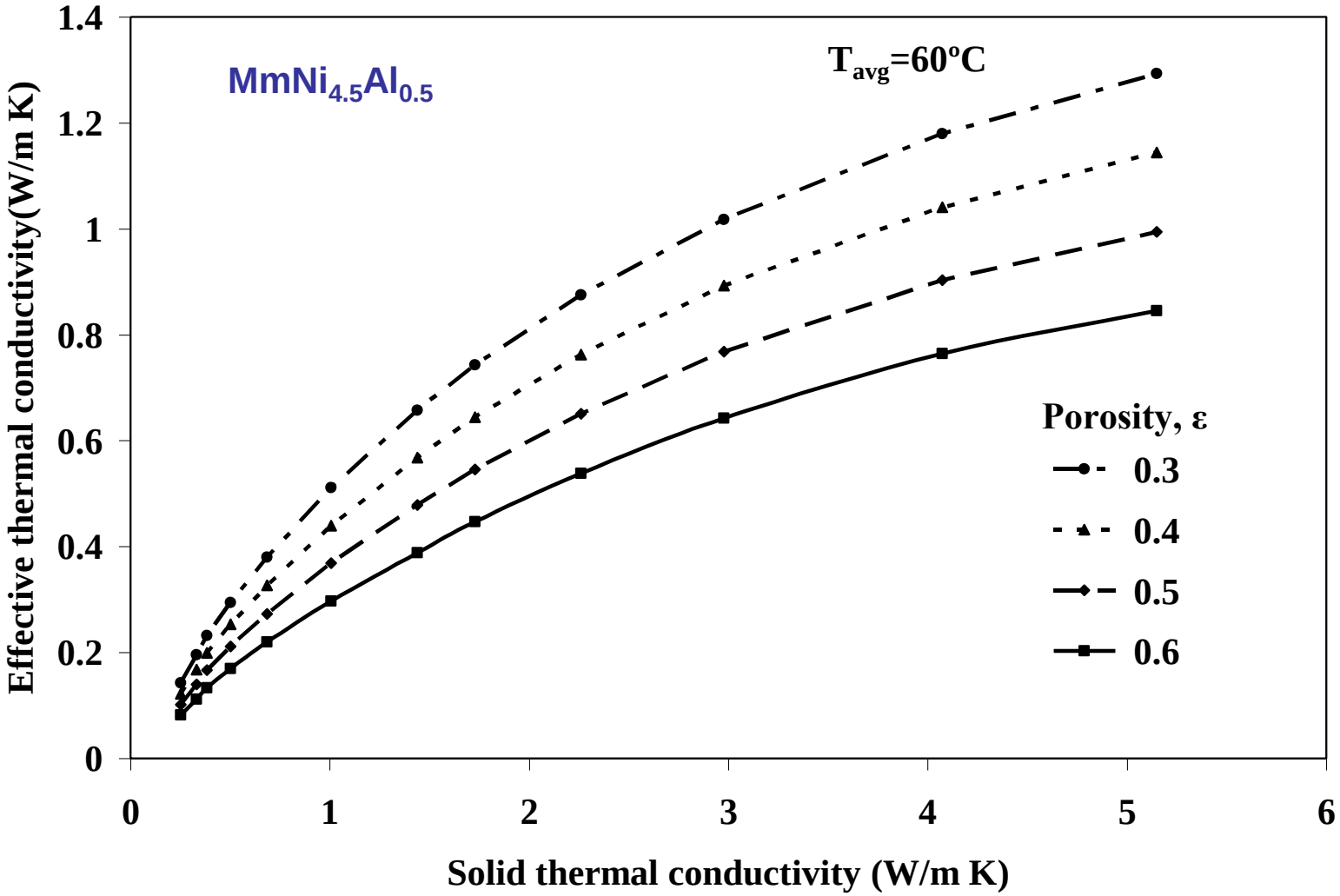

Variation of effective thermal conductivity of the bed with porosity

OBSERVATIONS

- **Effective thermal conductivity of metal hydride bed increases in the form of an tilted S shaped curve, low and nearly constant values at very low pressures, an intermediate region of steadily increasing conductivity with increasing pressure and nearly constant but high values at very high pressures.**
- **In the pressure dependent region the effective thermal conductivity is directly proportional to the value of gas thermal conductivity.**
- **The effective thermal conductivity increases with increasing hydrogen concentration. The increase is high in α region**
- **Effective solid thermal conductivity increases with hydrogen concentration similar to the variation of pressure in PCI curve.**

Augmentation Techniques

For portable and mobile hydrogen storage applications, heat transfer augmentation may prove to be counterproductive due to the added weight of high thermal conductivity materials which do not participate in hydrogen sorption.

It should be kept in mind that heat transfer augmentation improves the rates of hydrogen uptake and release but not the storage capacity.

Some of the methods adapted for improving the k_e of metal hydrides are:

- **Wire meshes (Copper or Aluminum)**
- **Foams**
- **Encapsulation**
- **Metal Matrix Composites**
- **Expanded Graphite or Carbon Fibres**

COMPLEX METAL HYDRIDES

- Alanates
- Borohydrides

General formula for alanates: $M(AlH_4)_n$

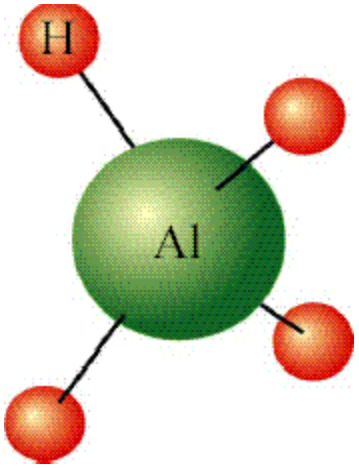

$NaAlH_4$ $LiAlH_4$ $Mg(AlH_4)_2$

$Ca(AlH_4)_2$ $KAlH_4$ $Ti(AlH_4)_4$

- Hydrogen atoms arranged tetrahedrally around Al
- Hydrogen retains significant hydride or electron-rich character

Estimated Hydrogen Storage Capacity

Hydride	H_2 Content (wt%)
$LiAlH_4$	10.5
$NaAlH_4$	7.5
$KAlH_4$	5.7
$Be(AlH_4)_2$	11.3
$Mg(AlH_4)_2$	9.3
$Ca(AlH_4)_2$	7.7
$Ti(AlH_4)_4$	9.3
$LiBH_4$	18.0
$NaBH_4$	10.4
$Al(BH_4)_3$	17.0

DECOMPOSITION REACTION

Two step process

$NaAlH_4 \longrightarrow 1/3\ Na_3AlH_6 + 2/3\ Al + H_2$

$Na_3AlH_6 \longrightarrow 3\ NaH + Al + 3/2\ H_2$

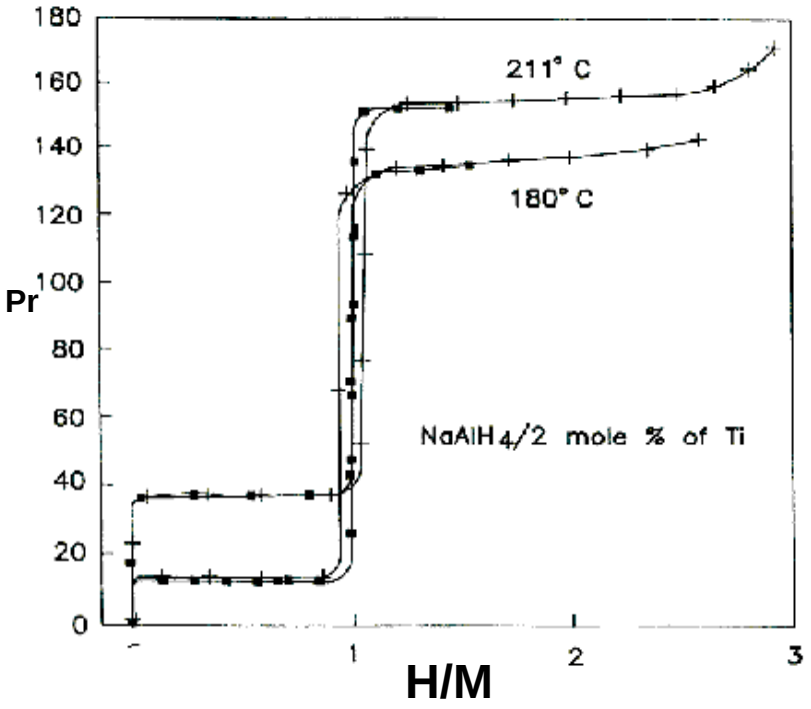

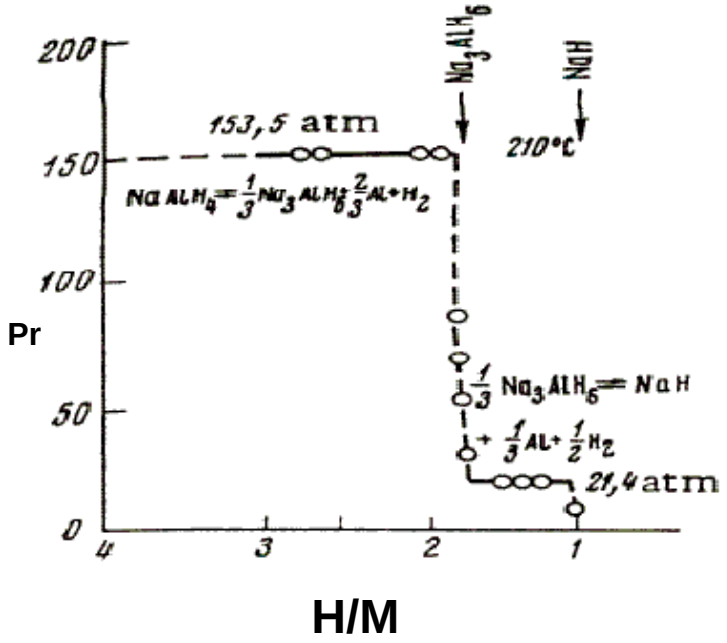

Reversibility

$NaAlH_4 + Ti(OBu)_4$ Ti doped $NaAlH_4$

$NaAlH_4 + TiCl_3$ Ti doped $NaAlH_4$

B. Bogdanovic and M. Schwickardi, *J. Alloys Comp.* 257 (**1997)** 1

Thermodynamics

$3\ NaAlH_4 \longrightarrow Na_3AlH_6 + 2\ Al + 3\ H_2$ (3.7 wt%) ; $\Delta H = +37$ kJ/mol

$Na_3AlH_6 \longrightarrow 3\ NaH + Al + 3/2\ H_2$ (1.9 wt%) ; $\Delta H = +47$ kJ/mol

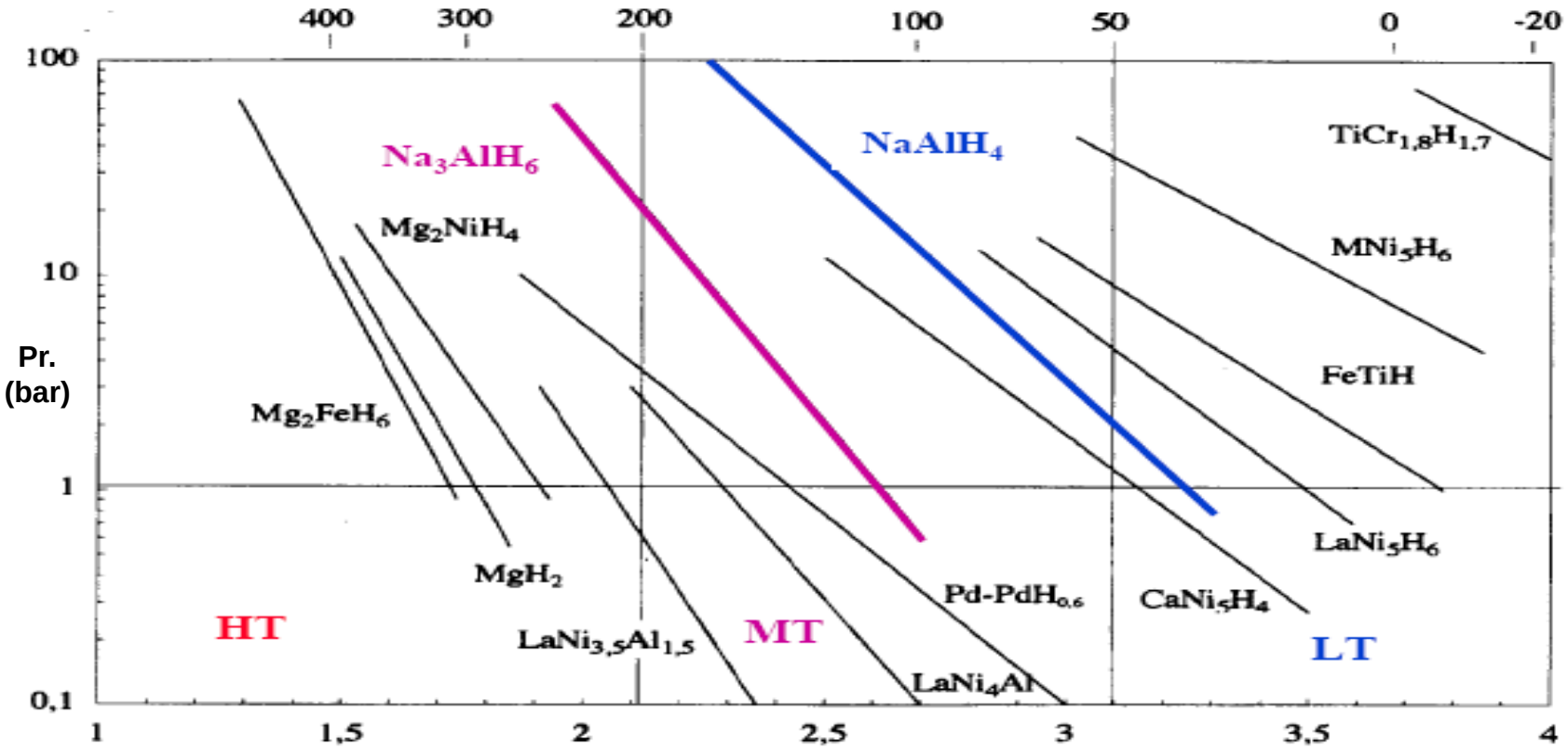

- $NaAlH_4$ is a low temperature hydride
- Na_3AlH_6 is the medium temperature hydride

B. Bogdanovic, Richard A. Brand, A. Marjanovic, M. Schwickardi and J. Tölle, *J. Alloys Comp.* 330-332 (2002) 683

$3\ NaAlH_4 \longrightarrow Na_3AlH_6 + 2\ Al + 3\ H_2\ (3.7\ wt\%)\ ;\ \Delta H = +37\ kJ/mol$

$Na_3AlH_6 \longrightarrow 3\ NaH + Al + 3/2\ H_2\ (1.9\ wt\%)\ ;\ \Delta H = +47\ kJ/mol$

Operating conditions

Coolant temp: 373 K
Supply pressure of H2 : 70 bar

Geometric parameters of the storage container with embedded HX tubes

Pitch distance : 24 mm
Tube diameter : 14 mm
Bed thickness : 5 mm

No.of HX tubes : 265

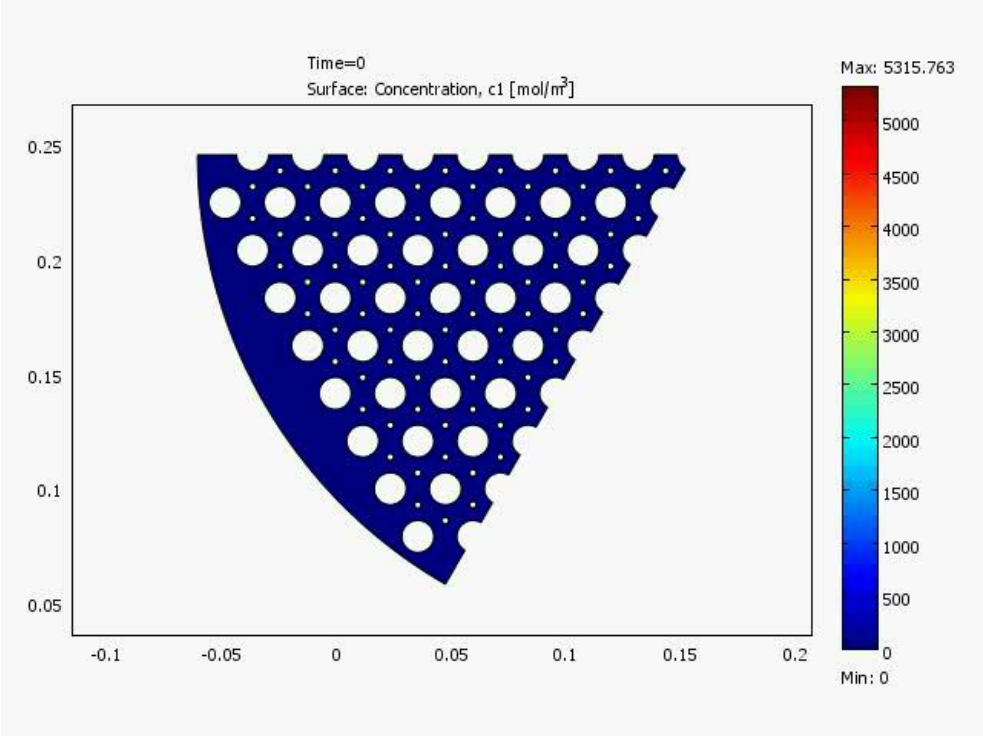

Kinetics : SRNL Report on "Integrated Hydrogen storage system Model" by Bruce J. Hardy

HYDROGEN STORAGE IN CARBON

•A variety of carbons like activated carbon, carbon nano tubes- multi walled (MWNT) and single-walled (SWNT), activated carbon fibers, graphitic nanofibers (GNF), carbon nanohorns have been studied for their hydrogen storage properties.

•The physisorption of hydrogen in these materials depends primarily on the pore size, generally classified as micropores (< 2 nm), mesopores (between 2 and 50 nm), and macropores (> 50 nm).

•Above critical point, adsorption takes place in micropores only and the density of adsorbed phase (in micropores) is much greater than that of unadsorbed gaseous phase (in macropores and slit volumes). Therefore, available micropore specific surface area plays vital role in deciding the adsorption capacity of the system.

•The hydrogen storage capacity depends upon type (granular, powder, pellet etc) of carbon and varies from 0.5 to 5 wt % at temperatures down to 77 K and pressures up to 100 bar.

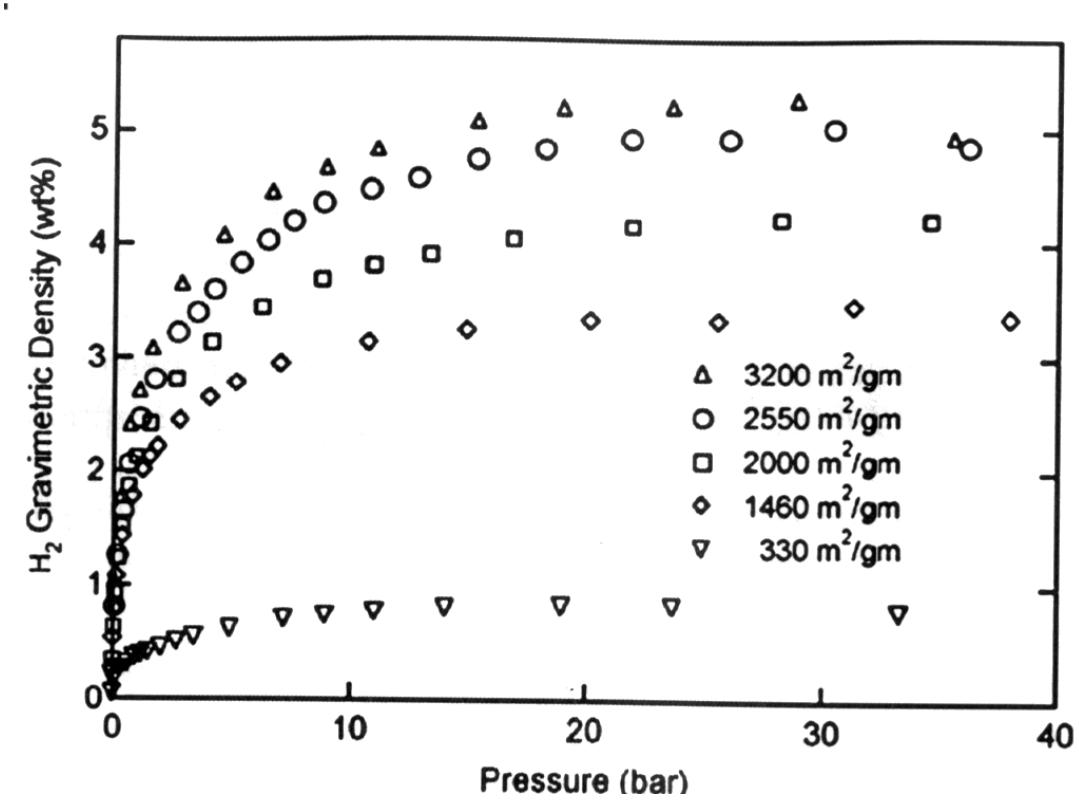

Adsorption isotherms at 77 K for carbon aerogels shows linear dependency of hydrogen uptake to the surface area. Increasing the surface area by a variety of means has been attempted.

GNF,SWNT,MWNT	**1.5%**	**1000 m2 /g**
Mesoporous carbon	**7 %**	**3200 m2 /g; 77 K , 20 bar**
Activated carbon fibres	**5%**	**77 K, 30 – 60 bar**
Carbon Aerogels	**5%**	**3200 m2 /g; 77 K , 20 bar**

Kabbour,H, Baumann,T.F.,Satcher,J.H.,Saulnier,A and Ahb\n,C.C., Chem, Mater.,18, p.6085, 2006

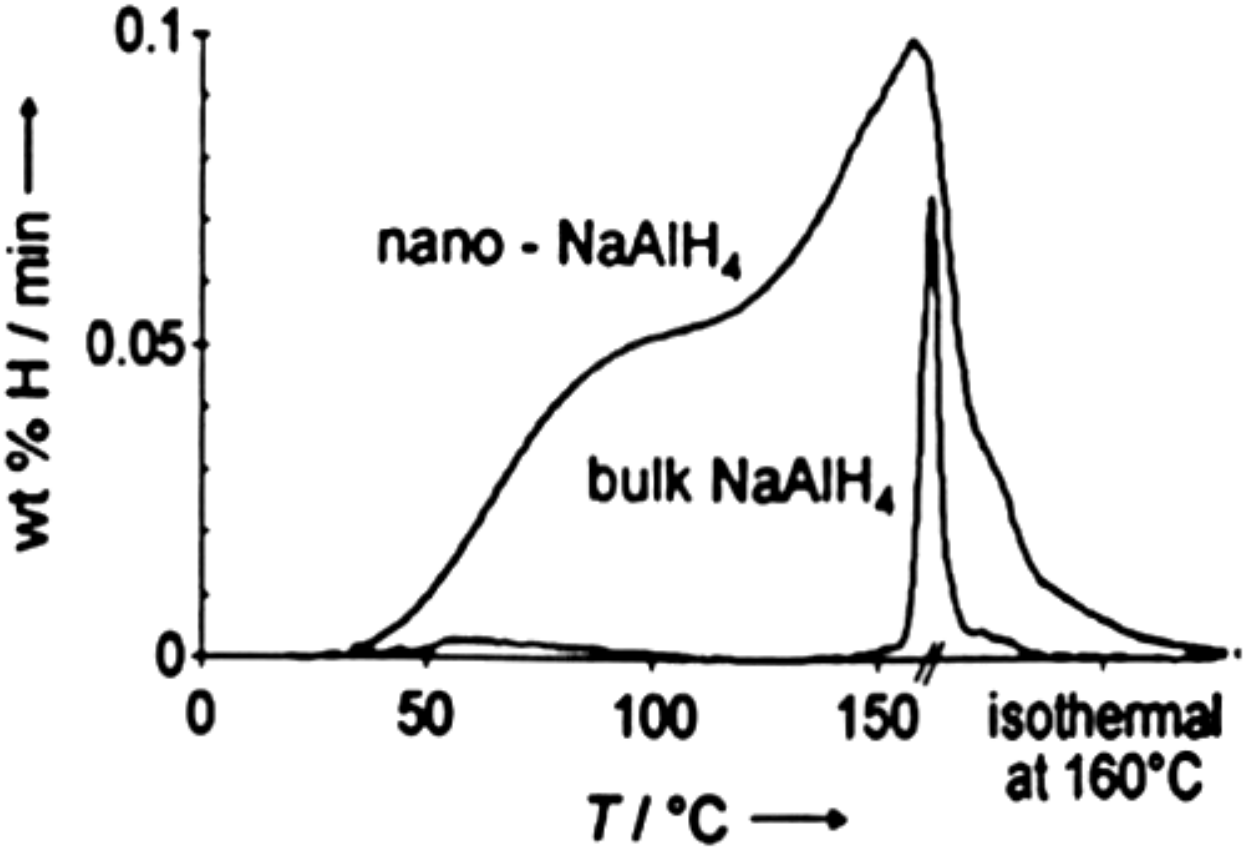

The improved hydrogen desorption for sodium alanate supported on carbon nanofibers

Balde,C.P., Herijgers,B.P.C., Bitter, J.H.,and de Jong,K.P., J.Am.Chem.Soc.,130, p.6761, 2008.

CLATHRATE HYDRATES

These are materials with structure formed by framework of H_2O molecules and guest molecules trapped inside of polyhedral cages. Hydrates of methane and natural gas are well known for many years and form large scale deposits in deep-sea sediments.

It was recognized recently that clathrate hydrates can be attractive materials for hydrogen storage applications.

Early reports of existence for H_2–H_2O clathrates have not attracted much attention from the point of view of hydrogen storage since the hydrate have been found only at very high pressures (0.75–2.3 GPa).

Recently, the pressure required for the formation of hydrogen clathrate hydrate has been lowered to 200 MPa (at temperatures below 250 K), which is still too high for any practical applications. Theoretical modeling and characterization of these clathrates have also been reported.

The real breakthrough for hydrogen storage applications have been reported recently for binary clathrate hydrate H_2O+H_2+THF. It has been claimed that hydrogen storage capacity of binary clathrate depends on THF content in the mixture and can be increased to 4 wt% for 0.15 mol% of THF.

Formation of this hydrogen clathrate hydrate has been observed at remarkably low pressures of only 150 bar (15 MPa) and at temperatures very close to the required room temperature interval (270 K).

If confirmed independently, hydrogen clathrates can be considered as a nearly ideal material for hydrogen storage applications. This material can adsorb hydrogen at temperatures slightly below room temperatures and release hydrogen simply upon heating the sample slightly above the melting point of $THF–H_2O$ with overall storage capacity of 4 wt%.

Feasibility of $H_2–THF–H_2O$ clathrate hydrates for hydrogen storage applications; Alexandr Talyzin; International Journal of Hydrogen Energy; Volume 33(1), 2008, pp.111-115

CONCLUDING REMARKS

Solid state hydrogen storage devices are of importance, especially for portable and mobile applications.

The thermal design of these devices involves the solution of transient coupled heat and mass transfer with heat generation and chemical reaction.

Important design considerations are gravimetric hydrogen storage capacity and charging / discharging rates of the device. A large number of geometric and operational parameters need to be taken into account.

Most of the analyses are macro-scale. Micro- and nano-scale modeling need to be done.

While a variety of storage materials have been suggested, there is a severe lack of data on thermodynamic and thermophysical properties.

CONCLUDING REMARKS

Due to the dynamic nature of charging and discharging processes, the properties vary continuously.

A key property is the effective thermal conductivity of the hydride bed which generally lies between 0.1 to 1.2 W/ m K in pressure and temperature ranges of 0 to 50 bar and 0 to 100ºC.

In the design of metal hydride devices the effect of hydrogen concentration and pressure on properties should be included.

In view of the low gravimetric storage capacity of metals and alloys, new complex hydrides such as alanates and borates are being suggested as storage media.

Thermal analyses of storage systems with these materials are rather rare as the reactions are more complex, and very little data is available on their thermodynamic and transport properties.

OTHER ISSUES

- **Hydrogen production**
- **Standards**
- **Economics**
- **Impact on carbon emissions**
- **Safety**
- **Applications**
- **Etc……..**

THANK YOU VERY MUCH

I HOPE THAT YOU LIKED THE

International Heat Transfer Conference IHTC14, August 8-13, 2010, Washington, DC, USA, Paper No. IHTC14-23345, "HEAT AND MASS TRANSFER ISSUES IN THE DESIGN OF SOLID STATE HYDROGEN STORAGE DEVICES"
Keynote Talk Delivered by me.
I can send a soft copy if you need. My e-mail: ssmurthy@iitm.ac.in